Phase diagram of the bosonic double-exchange model

J. L. Alonso,[1,2] A. Cruz,[1,2] L. A. Fernández,[3,2] S. Jiménez,[1,2] V. Martín-Mayor,[3,2] J. J. Ruiz-Lorenzo,[4,2] and A. Tarancón[1,2]

[1]*Departamento de Física Teórica, Facultad de Ciencias, Universidad de Zaragoza, 50009 Zaragoza, Spain*
[2]*Instituto de Biocomputación y Física de Sistemas Complejos (BIFI), Zaragoza, Spain*
[3]*Departamento de Física Teórica, Facultad de Ciencias Físicas, Universidad Complutense, 28040 Madrid, Spain*
[4]*Departamento de Física, Facultad de Ciencias, Universidad de Extremadura, 06071 Badajoz, Spain*
(Received 3 March 2004; revised manuscript received 22 July 2004; published 14 January 2005)

The phase diagram of the simplest approximation to double-exchange systems, the bosonic double-exchange model with antiferromagnetic (AFM) superexchange coupling, is fully worked out by means of Monte Carlo simulations, large-N expansions, and variational mean-field calculations. We find a rich phase diagram, with no first-order phase transitions. The most surprising finding is the existence of a segmentlike ordered phase at low temperature for intermediate AFM coupling which cannot be detected in neutron-scattering experiments. This is signaled by a maximum (a cusp) in the specific heat. Below the phase transition, only short-range ordering would be found in neutron scattering. Researchers looking for a quantum critical point in manganites should be wary of this possibility. Finite-size scaling estimates of critical exponents are presented, although large scaling corrections are present in the reachable lattice sizes.

I. INTRODUCTION

There are at least two motivations for studying the spin-only version of the double-exchange (DE) models. On the one hand, one has its relationship with the colossal magnetoresistance (CMR) effect.[1–3] On the other hand, in this problem some puzzles arise[4] with the universality hypothesis,[5] which deserve a detailed study. Let us start addressing the first aspect.

CMR has renewed the interest in double-exchange systems.[6] The typical CMR manganites are $La_{1-x}A_xMn_{1-y}O_3$, where A=Ca, Sr in the range $0.2 < x < 0.5$. It is believed that the relevant degrees of freedom[1] are the localized $S=3/2$ Mn^{3+} core spins, and the e_g holes. The Mn^{3+} ions form a single cubic lattice and, besides the DE mechanism, interact through an antiferromagnetic (AFM) superexchange coupling. The relatively high spin of the Mn^{3+} core suggests treating them as classical spins $\vec{\phi}_i$. Although phonons are believed to be crucial for the CMR effect,[7] manganites display a very rich magnetic phase diagram which can be addressed neglecting lattice effects.[8] In spite of these simplifications, and of the introduction of powerful new tools,[9–11] the numerical study of the DE model in large lattices beyond the mean-field approximation is out of reach for present day computers. Yet, finite-size effects in these systems are unusually large.[8] The need to obtain reliable predictions has made people further simplify models, replacing e_g holes by an effective interaction among the localized $S=3/2$ Mn^{3+} core spins. Indeed, a simple calculation[6] shows that the kinetic energy of the electrons depends on the relative orientation of neighboring Mn^{3+} core spins as $\sqrt{1+\vec{\phi}_i\vec{\phi}_j}$. This substitution of a simpler spin-only problem in place of the very difficult electronic problem lies at the heart of several theoretical analyses (see, e.g., de Gennes in Ref. 6) and numerical simulations.[12] In spite of this, to our knowledge there is only one detailed previous study[13] of the phase diagram of the bosonic DE model. That study predicted the existence of a

disordered paramagnetic (PM) phase at very low temperatures for intermediate superexchange coupling. This is very reminiscent of the presence of a quantum critical point[14] which is believed to be of importance for the CMR phenomenon,[15] and has been predicted to occur in manganites by some model calculations.[16] The experimental characterization of this quantum critical point is a wedge of paramagnetic phase, maybe glassy,[17] that at zero temperature becomes a single point separating two ordered phases.[15] The glassy wedge would be created by disorder,[15] and would be separated from the paramagnetic state at the high-temperature scale T^*. Maybe the most surprising result of the here presented analysis is that this glassy wedge could not be PM or glassy at all, but ordered in a segmentlike way[18–21] (as in liquid crystals). This ordering will be referred to in the following as RP^2 (real projective space). As we shall show, the RP^2 phase cannot be detected in neutron-scattering experiments (although a short-range ordering will be present). Nevertheless, the phase transition can be studied experimentally using the specific heat, which should present a maximum (furthermore, a cusp) at the critical temperature. Indeed, the thermal critical exponent is predicted[4] to be $\nu=0.78(2)$ which implies $\alpha=-0.34$, and hence the cusp behavior follows. Another bonus of our simplified model is that it allows us to study qualitatively (see Sec. IV D) the unusual interplay between ferromagnetism, antiferromagnetism, temperature, and applied magnetic field in low-doped $La_{1-x}Sr_xMnO_3$.[23–26]

Let us now address universality. A common wisdom is that the critical properties of a system are given by its dimensionality and the local properties (i.e., near the identity element) of the coset space $\mathcal{G}/\mathcal{H}$, where $\mathcal{G}$ is the symmetry group of the Hamiltonian (the symmetry of the high-temperature phase) and $\mathcal{H}$ is the remaining symmetry group of the broken phase (low temperature). So, systems with locally isomorphic $\mathcal{G}/\mathcal{H}$ belong to the same universality class. This seems to be true in perturbation theory, where the ob-

servables are computed by doing series expansions around the identity element of $\mathcal{G}/\mathcal{H}$. In this picture, a phase transition of a vector model, with O(3) global symmetry and with an O(2) low-temperature phase symmetry, in three dimensions must belong to the O(3)/O(2) scheme of symmetry breaking (classical Heisenberg model). In addition, if $\mathcal{H}$ =O(1)=Z_2 is the remaining symmetry, the corresponding scheme should be[27] O(4)/O(3) which is locally isomorphic to O(3)/O(1).

Hence, it is interesting to check if the global properties of the coset space $\mathcal{G}/\mathcal{H}$ are relevant or not to the phase transition. The common wisdom has been challenged in the past by the so-called chiral models.[28] However, the situation is still hotly debated: some authors believe that the chiral transitions are weakly first order,[29] while others claim[30] that the chiral universality class exists, implying the relevance of the global properties of $\mathcal{G}/\mathcal{H}$. On the other hand, we do not have any doubt about the second-order nature of the PM−RP^2 transition. A detailed study of the critical exponents was recently published[4] in letter form. In the present work, we perform a detailed Monte Carlo, mean field, and large-N study of the phase diagram. The large-N calculation is actually split into two different computations (for $J < -1/2$ and $J > -1/2$); therefore, there are two different saddle points for the paramagnetic phase. A thorough study is performed of the RP^2 phase. We shall confirm that the pattern of symmetry breaking is O(3)/O(2), suggesting a violation of universality. However, a qualitative argument (see Sec. IV B) suggests that the universality class could be the one of the O(5) nonlinear σ model. Indeed, the numerical results are compatible with this possibility.

The layout of the rest of this paper is as follows. In Sec. II we define the model, study the phase diagram at zero temperature, and define the order parameters and observables measured in the Monte Carlo simulations. The mean-field calculation is explained in Sec. III, where we also report the results of the large-N analysis. In Sec. IV we present our Monte Carlo results. We start determining the global phase diagram in Sec. IV A. What is known[19] about a generic RP^2 phase is recalled in Sec. IV B. The RP^2 phase, as realized in the double-exchange model, is investigated in more detail in Sec. IV C, while the effects of a magnetic field on conductivity close to a ferromagnetic-antiferromagnetic transition are considered in Sec. IV D. We present our conclusions in Sec. V. We complement the paper with three appendixes. Appendix A contains the details about the large-N calculation. In Appendix B the reader will find the mean-field phase diagram as obtained from the fourth-order expansion of the free energy. Finally, in Appendix C a spin-wave calculation for the low-temperature RP^2 region is presented.

II. THE MODEL

A. The Hamiltonian

We define a system of spins $\{\vec{\phi}_i\}$ existing in a three-dimensional cubic lattice of size L (and volume $V = L^3$) with periodic boundary conditions. The spins are three-component real unit vectors. We consider the Hamiltonian

$$H = -\sum_{\langle i,j \rangle} \left(J\vec{\phi}_i \cdot \vec{\phi}_j + \sqrt{1 + \vec{\phi}_i \cdot \vec{\phi}_j} \right), \tag{1}$$

where the sum is extended to all pairs of nearest neighbors and we consider only $J < 0$. Notice that we will measure temperature in units of the double-exchange constant. The cubic lattice is bipartite; therefore we shall call the lattice site i *even* or *odd* according to the parity of the sum of its coordinates, $x_i + y_i + z_i$.

We will consider the system at a temperature T, the partition function being

$$Z = \int \prod_i d\vec{\phi} \, e^{-H/T}, \tag{2}$$

where the integration measure is the standard measure on the unit sphere.

B. Phase diagram at zero temperature

As usual, the study of the phase diagram begins with an understanding of the ordered phases at zero temperature. We can write in a compact way our original Hamiltonian:

$$H = -\sum_{\langle i,j \rangle} \mathcal{V}(\vec{\phi}_i \cdot \vec{\phi}_j), \tag{3}$$

where

$$\mathcal{V}(y) = Jy + \sqrt{1 + y}, \tag{4}$$

and clearly $y \in [-1, 1]$. In the limit of zero temperature, the only configurations that contribute to the partition function are those that provide a maximum of $\mathcal{V}(y)$. If, as confirmed by the Monte Carlo simulations, the spin texture itself is bipartite, the value of y will be uniform through the lattice. Thus, a simple computation yields that the maxima of $\mathcal{V}(y)$ are at the following values of y (denoted by y_{max}):

$$y_{max} = \begin{cases} 1 & \text{for } J \geq -\dfrac{1}{2\sqrt{2}}, \\ -1 + \dfrac{1}{4J^2} & \text{for } J \leq -\dfrac{1}{2\sqrt{2}}. \end{cases} \tag{5}$$

It is clear that $y_{max} = 1$ corresponds to a ferromagnetic state and that in the $J \to -\infty$ limit we reach an anti-ferromagnetic one ($y_{max} = -1$). The intermediate values of y_{max} correspond to a ferrimagnet if $0 < y_{max} < 1$ and to an antiferrimagnet when $-1 < y_{max} < 0$. The physical picture is as follows. The spins in the, say, even sublattice are all parallel along (for instance) the Z axis. On the other hand the odd spins lie on a cone forming an angle θ ($\cos \theta = y_{max}$) with the Z axis.

The corresponding free energy is just

$$f(J) = \begin{cases} \sqrt{2} + J & \text{for } J \geq -\dfrac{1}{2\sqrt{2}}, \\ -\dfrac{1}{4J} - J & \text{for } J \leq -\dfrac{1}{2\sqrt{2}}. \end{cases} \tag{6}$$

Hence we have the following phase transitions.

(1) *Ferromagnetic-ferrimagnetic* at $J = -1/\sqrt{8}$. It is easy

to check that df/dJ is continuous at $J=-1/\sqrt{8}$ but d^2f/dJ^2 is discontinuous. Hence, according to the standard Erhenfest classification, we have a second-order phase transition.

(2) *Ferrimagnetic-antiferrimagnetic* at $J=-1/2$, where the free energy is C^∞. At this special point y_{max} changes from positive to negative. The fact that $y_{max}=0$ implies that one can reverse every single spin independently of the others without changing the energy (more pedantically, one finds a dynamically generated Z_2 gauge symmetry[4]).

(3) The limiting value $y_{max}=-1$ that corresponds to an *antiferromagnet* rather than an antiferrimagnet is reached only at $J=-\infty$.

The transition 2 (ferrimagnet-antiferrimagnet) needs further discussion. We can expand the Hamiltonian around the minimum $y=0$, and we obtain

$$\mathcal{V}(y) = 1 - \frac{1}{8}y^2 + O(y^3). \tag{7}$$

Thus, at $J=-0.5$ and close to $T=0$ one has, neglecting constant terms,

$$H = \frac{1}{8}\sum_{\langle i,j\rangle}(\vec{\phi}_i \cdot \vec{\phi}_j)^2 + O((\vec{\phi}_i \cdot \vec{\phi}_j)^3), \tag{8}$$

which corresponds to an antiferromagnetic RP^2 theory.[18–21] The minimum energy configuration satisfies $y=0$. Hence, we obtain that the ferrimagnet-antiferrimagnet transition occurs at zero temperature via a RP^2 state at a single point. We shall see that at finite temperature the RP^2 phase occupies a region close to $J=-0.5$ (rather than a single point) of the phase diagram.

From the previous analysis at zero temperature, one expects to find the following phases at finite temperature.

PM: the usual disordered state, where all the symmetries of the model are preserved.

FM: a standard ferromagnetic ordering, i.e., the spin fluctuates around $(0,0,1)$.

AFM: a standard antiferromagnetic ordering. Even (odd) spins fluctuate around $\vec{\phi}^e=(0,0,1)$ [$\vec{\phi}^o=(0,0,-1)$].

FI: The ordering consists on even spins fluctuating around the Z axis and odd spins fluctuating around the cone of angle $\theta<\pi/2$ with axis Z.

AFI: This ordering is similar to the previous one, with $\theta > \pi/2$.

RP²: Here the ordering is the finite-T version of the one found analytically in $J=-0.5$, $T=0$, i.e., even spins fluctuating around the Z axis with random sense, and odd spins fluctuating around the cone with random sense.

C. Order parameters

In models with antiferromagnetic couplings, one might expect an even-odd structure of the ordered phases. Therefore, from the local field $\{\vec{\phi}_i\}$, we define the standard magnetization as the Fourier transform at momentum 0, and the staggered magnetization as the Fourier transform at momentum (π,π,π):

$$\vec{M} = \frac{1}{L^3}\sum_i \vec{\phi}_i, \tag{9}$$

$$\vec{M}_s = \frac{1}{L^3}\sum_i (-1)^{x_i+y_i+z_i}\vec{\phi}_i. \tag{10}$$

In a finite lattice we must take the modulus before taking the mean value. We will study

$$\mu^V = \langle\|\vec{M}\|\rangle, \tag{11}$$

$$\mu_s^V = \langle\|\vec{M}_s\|\rangle. \tag{12}$$

The associated susceptibilities are

$$\chi^V = L^3\langle\vec{M}^2\rangle, \tag{13}$$

$$\chi_s^V = L^3\langle\vec{M}_s^2\rangle. \tag{14}$$

In order to explore RP^2-type phases we introduce a tensor invariant under the local spin reversal. In this case we use as local field the matrices $\{\tau_i\}$, constructed as

$$\tau_i = \phi_i^\alpha\phi_i^\beta - \frac{1}{3}\delta^{\alpha\beta}, \quad \alpha,\beta=1,2,3. \tag{15}$$

Notice that they are traceless; thus they represent objects of spin 2. We can now define the associated traceless tensor magnetizations

$$\mathsf{M} = \frac{1}{L^3}\sum_i \tau_i, \tag{16}$$

$$\mathsf{M}_s = \frac{1}{L^3}\sum_i (-1)^{x_i+y_i+z_i}\tau_i, \tag{17}$$

and the mean values

$$\mu^T = \langle\sqrt{\mathrm{Tr}\,\mathsf{M}^2}\rangle, \tag{18}$$

$$\mu_s^T = \langle\sqrt{\mathrm{Tr}\,\mathsf{M}_s^2}\rangle. \tag{19}$$

The corresponding susceptibilities are

$$\chi^T = L^3\langle\mathrm{Tr}\,\mathsf{M}^2\rangle, \tag{20}$$

$$\chi_s^T = L^3\langle\mathrm{Tr}\,\mathsf{M}_s^2\rangle. \tag{21}$$

Let us close this subsection by recalling the value's of the order parameters (in the infinite-volume limit) in each of the ordered phases found in the previous subsection:

FM: $\mu^V > 0$, $\mu_s^V = 0$ ($\Rightarrow \mu^T > 0$, $\mu_s^T = 0$),

AFM: $\mu_s^V > 0$, $\mu^V = 0$ ($\Rightarrow \mu^T > 0$, $\mu_s^T = 0$),

FI: $\mu^V > \mu_s^V > 0$ ($\Rightarrow \mu^T$, $\mu_s^T > 0$),

AFI: $\mu_s^V > \mu^V > 0$ ($\Rightarrow \mu^T$, $\mu_s^T > 0$),

RP²: $\mu_s^T > \mu^T > 0$, $\mu_s^V = \mu^V = 0$. $\qquad$ (22)

D. Correlation length

In the most general case, for models with antiferromagnetic interactions, both the usual susceptibility and also the staggered susceptibility diverge. Thus, in the Brillouin zone, one needs to monitor the behavior of the Green functions close to the origin as well as close to (π, π, π). Since in critical-phenomena studies one usually considers only the behavior around zero momentum, it is more intuitive—although redundant—to define four Green functions in terms of four fields in momentum space:

$$\hat{\vec{\phi}}(\boldsymbol{p}) = \sum_i e^{-i\boldsymbol{p}\cdot\boldsymbol{r}_i}\vec{\phi}_i, \tag{23}$$

$$\hat{\vec{\phi}}_s(\boldsymbol{p}) = \sum_i e^{-i\boldsymbol{p}\cdot\boldsymbol{r}_i}(-1)^{x_i+y_i+z_i}\vec{\phi}_i, \tag{24}$$

$$\hat{\mathsf{T}}(\boldsymbol{p}) = \sum_i e^{-i\boldsymbol{p}\cdot\boldsymbol{r}_i}\tau_i, \tag{25}$$

$$\hat{\mathsf{T}}_s(\boldsymbol{p}) = \sum_i e^{-i\boldsymbol{p}\cdot\boldsymbol{r}_i}(-1)^{x_i+y_i+z_i}\tau_i, \tag{26}$$

the Fourier transforms of the correlation functions being

$$\hat{G}^V(\boldsymbol{p}) = \frac{1}{L^3}\langle\hat{\vec{\phi}}(\boldsymbol{p})\cdot\hat{\vec{\phi}}^*(\boldsymbol{p})\rangle, \tag{27}$$

$$\hat{G}_s^V(\boldsymbol{p}) = \frac{1}{L^3}\langle\hat{\vec{\phi}}_s(\boldsymbol{p})\cdot\hat{\vec{\phi}}_s^*(\boldsymbol{p})\rangle, \tag{28}$$

$$\hat{G}^T(\boldsymbol{p}) = \frac{1}{L^3}\langle\operatorname{Tr}\hat{\mathsf{T}}(\boldsymbol{p})\hat{\mathsf{T}}^\dagger(\boldsymbol{p})\rangle, \tag{29}$$

$$\hat{G}_s^T(\boldsymbol{p}) = \frac{1}{L^3}\langle\operatorname{Tr}\hat{\mathsf{T}}_s(\boldsymbol{p})\hat{\mathsf{T}}_s^\dagger(\boldsymbol{p})\rangle. \tag{30}$$

Notice that $\hat{G}_s^{V,T}(\boldsymbol{p}) = \hat{G}^{V,T}(\boldsymbol{p}+(\pi,\pi,\pi))$, so that one could consider only nonstaggered correlation functions that would be studied close to both $(0, 0, 0)$ and (π, π, π).

Near a (continuous) phase transition where the corresponding correlation length ξ diverges, the correlation functions in the thermodynamic limit behave for small $\boldsymbol{p}^2\xi^2$, as

$$\hat{G}(\boldsymbol{p}) \simeq \frac{Z\xi^{-\eta}}{\boldsymbol{p}^2+\xi^{-2}}. \tag{31}$$

Here ξ diverges as $|t|^{-\nu}$, t being the reduced temperature. The anomalous dimension η will depend on the considered field.

In a finite lattice, to estimate the correlation length one uses the propagator at zero momentum and at the minimum nonzero momentum compatible with boundary conditions. Defining $F=\hat{G}(2\pi/L,0,0)$ and noting that $\chi=\hat{G}(0)$, one has[31]

$$\xi = \left(\frac{\chi/F-1}{4\sin^2(\pi/L)}\right)^{1/2}. \tag{32}$$

III. MEAN-FIELD CALCULATION

When several phases compete, it is quite tricky to calculate the phase diagram in the mean-field approximation (the $T=0$ calculation has shown that we should face this problem). Since one can find different ordered phases at low temperatures within different mean-field schemes, it is necessary to decide which phase will be the most stable one. We consider that the cleanest way of performing such a calculation is to use the variational formulation of the mean-field approximation (see, for example, Ref. 32), with a variational family large enough to take into account all the phases found in the phase diagram. In this way, all the phases compete on the same grounds and one has an objective criterion to decide which phase is to be found in a given region of the phase diagram.

One needs to compare the actual system with a simplified model where all degrees of freedom are statistically independent. The method is derived from the inequality[32]

$$F \leq F_0 + \langle H - H_0\rangle_0. \tag{33}$$

Here, H_0 is a trial Hamiltonian depending on some parameters (the *mean fields*) and the average $\langle\ldots\rangle_0$ means the average with the Boltzmann weight corresponding to H_0. The right-hand side of the inequality (33) is minimized with respect to the free parameters in H_0 and then used as our best estimate of the free energy. Thus the task is to generalize the standard Curie-Weiss ansatz $H_0=h\Sigma_i\phi_i^z$ (ϕ_i^z is the component of the local spin $\vec{\phi}_i$ along the Z axis), to cover all the expected orderings.

In our case, we must use the simplest possible variational family that permits us to have different orderings in the even and odd sublattices:

$$H_0 = -\sum_{i\,\text{even}} V_e(\phi_i^z) - \sum_{i\,\text{odd}} V_o(\phi_i^z). \tag{34}$$

Notice that, as far as the calculation of the $\langle\cdots\rangle_0$ averages is concerned, all spins can be considered as statistically independent. Thus, the mean value of an arbitrary function of a spin placed in (say) the odd sublattice is simply

$$\langle f(\vec{\phi})\rangle_0^{(\text{odd})} = \frac{\displaystyle\int_0^{2\pi} d\varphi \int_{-1}^1 d\phi^z f(\vec{\phi})e^{-V_o(\phi^z)/T}}{\displaystyle\int_0^{2\pi} d\varphi \int_{-1}^1 d\phi^z e^{-V_o(\phi^z)/T}}, \tag{35}$$

$$\vec{\phi} = \left(\sqrt{1-(\phi^z)^2}\,\cos\varphi, \quad \sqrt{1-(\phi^z)^2}\,\sin\varphi, \phi^z\right). \tag{36}$$

We now need to parametrize the local potentials with the help of the mean fields, which will be our minimizing parameters. One easily sees that keeping only the linear term $[V_{e,o}(\phi^z)=h_{e,o}\phi^z]$ will not reproduce the ferrimagnetic or antiferrimagnetic phases, since at very low temperatures and nonvanishing mean fields $h_{e,o}$ the spins would always be (anti)aligned with the Z axis. If one keeps also the quadratic term $V_{e,o}(\phi^z)=h_{e,o}\phi^z+\lambda_{e,o}(\phi^z)^2$, the situation improves significantly. The minimum of $V_{e,o}$ can now be $-1 \leq \phi_{\min}^z \leq 1$ which implies that at low temperature spins would lie on the

cone of angle θ, $\cos \theta = \phi_{\min}^z$. Therefore, we will choose as our variational family

$$H_0 = -\sum_{i \text{ even}} \left[h_e \phi_i^z + \lambda_e (\phi_i^z)^2 \right] - \sum_{i \text{ odd}} \left[h_o \phi_i^z + \lambda_o (\phi_i^z)^2 \right].$$
(37)

As an extra bonus, we find that the RP^2 phase can be represented by this ansatz if the mean fields that minimize the right-hand side (RHS) of inequality (33)—at those particular T and J values—happen to be $h_e = h_o = 0$, $\lambda_e = -\lambda_o > 0$. This can be explicitly checked by calculating the order parameters as a function of the mean fields. Due to the symmetry between the even and odd sublattices, the expressions simplify in terms of the natural linear combinations of the mean fields h_e, h_o, λ_e, λ_o:

$$h = (h_e + h_o)/2,$$

$$h_s = (h_e - h_o)/2,$$

$$\lambda = (\lambda_e + \lambda_o)/2,$$

$$\lambda_s = (\lambda_e - \lambda_o)/2.$$
(38)

In terms of these variables, by means of a series expansion in h, h_s, λ, and λ_s, one gets for the order parameters

$$\mu^V = \frac{1}{2} \left(\langle \phi^z \rangle_0^{(\text{even})} + \langle \phi^z \rangle_0^{(\text{odd})} \right)$$

$$= \frac{2}{3} \beta h + \frac{8}{45} (h\lambda + h_s \lambda_s) + O(h^2, h_s^2, \lambda^2, \lambda_s^2),$$
(39)

$$\mu_s^V = \frac{1}{2} \left(\langle \phi^z \rangle_0^{(\text{even})} - \langle \phi^z \rangle_0^{(\text{odd})} \right)$$

$$= \frac{2}{3} \beta h_s + \frac{8}{45} (h_s \lambda + h \lambda_s) + O(h^2, h_s^2, \lambda^2, \lambda_s^2),$$
(40)

$$\mu^T = \frac{1}{2} \left[\langle (\phi^z)^2 \rangle_0^{(\text{even})} + \langle (\phi^z)^2 \rangle_0^{(\text{odd})} \right] - \frac{1}{3}$$

$$= \frac{4}{45} \beta \lambda + \frac{2}{45} \beta^2 (h^2 + h_s^2) + \frac{4}{945} \beta^2 (\lambda^2 + \lambda_s^2)$$

$$+ O(h^2, h_s^2, \lambda^2, \lambda_s^2),$$
(41)

$$\mu_s^T = \frac{1}{2} \left[\langle (\phi^z)^2 \rangle_0^{(\text{even})} - \langle (\phi^z)^2 \rangle_0^{(\text{odd})} \right]$$

$$= \frac{4}{45} \beta \lambda_s + \frac{1}{45} \beta^2 h h_s + \frac{8}{945} \beta^2 \lambda \lambda_s$$

$$+ O(h^2, h_s^2, \lambda^2, \lambda_s^2).$$
(42)

With this information in hand one can identify the different phases that we found at $T=0$ in terms of the nonvanishing mean fields (of course the high-temperature PM phase corresponds to the vanishing of all four mean fields):

FM: $\quad h > 0, \quad h_s = \lambda = \lambda_s = 0,$

AFM: $\quad h_s > 0, \quad h = \lambda = \lambda_s = 0,$

FI: $\quad h, \lambda_s > 0, \quad h_s = \lambda = 0,$

AFI: $\quad h_s, \lambda > 0, \quad h = \lambda_s = 0,$

RP^2: $\quad \lambda_s > 0, \quad h = h_s = \lambda = 0.$
(43)

Let us now describe the actual calculation. As previously said, we introduce the function

$$\Phi(h, h_s, \lambda, \lambda_s) = F_0 + \langle H - H_0 \rangle_0,$$
(44)

which, at its minimum as a function of h, h_s, λ, and λ_s, we shall identify (in mean-field approximation) with the equilibrium free energy. The partition function can be factorized to the contribution of the $V/2$ points of the even sublattice and the $V/2$ points of the odd sublattice:

$$Z_0 = Z_e^{V/2} Z_o^{V/2} = e^{-\beta F_0},$$
(45)

where

$$Z_{e,o} = \int_0^{2\pi} d\varphi \int_{-1}^1 d\phi^z e^{\beta \left[h_{e,o} \phi^z + \lambda_{e,o} (\phi^z)^2 \right]},$$
(46)

$$F_0 = -\frac{V}{2\beta} (\ln Z_e + \ln Z_o).$$
(47)

The average of the mean-field Hamiltonian is

$$\langle H_0 \rangle_0 = -\frac{V}{2} \left[h_e \langle \phi^z \rangle_0^{(\text{even})} + \lambda_e \langle (\phi^z)^2 \rangle_0^{(\text{even})} \right.$$

$$\left. + h_o \langle \phi^z \rangle_0^{(\text{odd})} + \lambda_o \langle (\phi^z)^2 \rangle_0^{(\text{odd})} \right].$$
(48)

As for the average of the true Hamiltonian, one finds

$$\langle H \rangle_0 = -3VJ \langle \phi^z \rangle_0^{(\text{even})} \langle \phi^z \rangle_0^{(\text{odd})} - 3VJ \left\langle \sqrt{1 + \vec{\phi}_e \cdot \vec{\phi}_o} \right\rangle_0.$$
(49)

In the above expression, $\vec{\phi}_{e,o}$ is a generic spin belonging to the even (odd) sublattice. The problem is that, even if $\vec{\phi}_e$ and $\vec{\phi}_o$ are statistically independent, the calculation of the mean value of the square root in Eq. (49) cannot be straightforwardly factorized in to even and odd contributions. In order to achieve this factorization, we shall use the series expansions introduced by de Gennes.[33] One first uses an expansion in Legendre polynomials:

$$\sqrt{1 + \vec{\phi}_e \cdot \vec{\phi}_o} = \sum_{l=0}^{\infty} A_l P_l (\vec{\phi}_e \cdot \vec{\phi}_o),$$
(50)

$$A_l = (-1)^{l+1} \frac{2\sqrt{2}}{(2l-1)(2l+3)}.$$
(51)

We can now factorize the Legendre polynomials using their expression in terms of spherical harmonics:
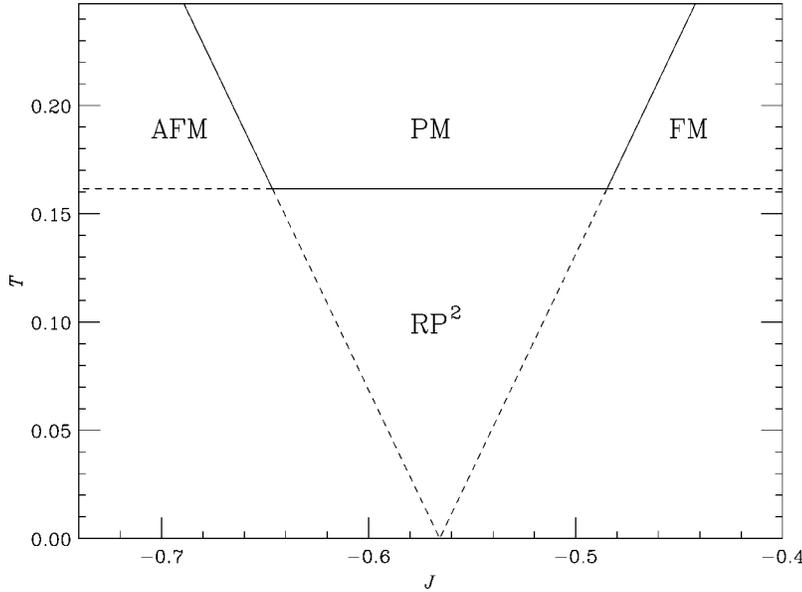
FIG. 1. Phase diagram as obtained from the second-order series expansion of the free energy (55). The paramagnetic phase is unstable for temperatures below the full lines (the instability being toward the FM, AFM, or RP^2 phase, as indicated in the plot). The dashed lines indicate the places where some of the eigenvalues of the quadratic form in Eq. (55) vanish, but they do not correspond to phase transitions.

$$P_l(\vec{\phi}_e \cdot \vec{\phi}_o) = \frac{4\pi}{2l+1} \sum_{m=-l}^{l} Y_l^{m*}(\phi_e^z, \varphi_e) Y_l^m(\phi_o^z, \varphi_o). \quad (52)$$

Thus, the mean values are factorized into even and odd contributions. Due to the rotational symmetry along the Z axis, only the $m=0$ terms in Eq. (52) are nonvanishing. Thus we obtain

$$\langle P_l(\vec{\phi}_e \cdot \vec{\phi}_o) \rangle_0 = \langle P_l(\phi^z) \rangle_0^{(\text{even})} \langle P_l(\phi^z) \rangle_0^{(\text{odd})}. \quad (53)$$

Fortunately, if one wants to calculate the free energy Φ as a series expansion in the mean fields h, h_s, λ, and λ_s at a given order only a finite number of terms in Eq. (50) contribute, due to the orthogonality properties of the Legendre polynomials. This expansion allows as to discuss the continuous phase transitions from the PM phase (where $h=h_s=\lambda=\lambda_s=0$ is the absolute minimum of the free energy) to ordered phases. Indeed, calculating Φ (per unit volume) to second order one gets

$$\frac{1}{V}\Phi(h,h_s,\lambda,\lambda_s) \approx \left(\frac{\beta}{6} - \frac{J\beta^2}{3} - \frac{2\sqrt{2}\beta^2}{15} \right)h^2$$

$$+ \left(\frac{\beta}{6} + \frac{J\beta^2}{3} + \frac{2\sqrt{2}\beta^2}{15} \right)h_s^2$$

$$+ \left(\frac{8\sqrt{2}\beta^2}{1575} + \frac{2\beta}{45} \right)\lambda^2$$

$$+ \left(-\frac{8\sqrt{2}\beta^2}{1575} + \frac{2\beta}{45} \right)\lambda_s^2. \quad (54)$$

This is a quadratic form in h, h_s, λ, and λ_s. If the above quadratic form is positive definite, the PM phase is a (local) minimum of the free energy. The other way around, when one of the eigenvalues of the quadratic form is negative, the PM phase is unstable with respect to some ordered phase, depending on the mean-field that should grow in order to minimize the free energy. Notice also that the eigenvalue

corresponding to λ^2 is always positive. Thus, even if there are four eigenvalues, we obtain three lines of continuous phase transitions, where the eigenvalues vanish:

$$\text{PM-FM line:} \quad T = 2J + 4\sqrt{2}/5,$$

$$\text{PM-AFM line:} \quad T = -2J - 4\sqrt{2}/5,$$

$$\text{PM-RP2 line:} \quad T = 4\sqrt{2}/35. \quad (55)$$

Therefore the PM phase, stable at high temperature, meets two transition lines of opposite slope, and a horizontal line that separates it from the RP2 phase (see Fig. 1).

For temperatures below the full lines in Fig. 1, one needs to discuss the stability of a minimum of the free energy different from $h=h_s=\lambda=\lambda_s=0$. To locate that minimum, and to discuss its stability, one needs to extend the series expansion in (55) at least to fourth order in h, h_s, λ, and λ_s. This can be done (see Appendix B), but it is not particularly illuminating since the series expansion for Φ is slowly convergent. We have rather turned to a numerical method. Given a particular value of the mean fields h, h_s, λ, λ_s, we have calculated Φ by means of a Gauss-Legendre integration of all the terms in Eq. (44). To do this, we have divided the interval $[-1, 1]$ into 12 subintervals and we have done a 12th-order Gauss-Legendre integration in each of them. The series of Eq. (50) has been evaluated to order 50. Being able to calculate Φ, the minimization has been done using a conjugate gradient method. The resulting phase diagram is shown in Fig. 2. It can be compared with the Monte Carlo data (see Fig. 1 of Ref. 4). The mean-field calculation overestimates the critical temperatures by (roughly) a factor 2.3. Once this factor is corrected the agreement between Monte Carlo and mean-field critical lines is remarkable.

The mean-field calculation predicts that all the transitions are second order except the ferromagnetic-RP2 which is first order (nevertheless, this transition line is an artifact of the mean-field solution; in the Monte Carlo phase diagram it seems to collapse to a tetracritical point, as shown in Fig. 1
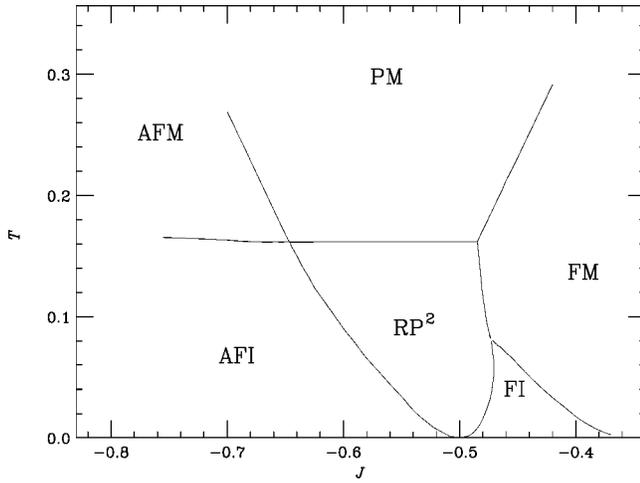
FIG. 2. Phase diagram of the model, as predicted by the Mean-Field approximation. The critical lines are obtained minimizing numerically the free-energy (44) (see text for details).

of Ref. 4). The second-order nature of the transitions found in the numerical minimization can be checked by computing the appropriate order parameter at a given value of T and J, then noticing that it vanishes at the transition line with mean-field exponents ($M \propto |T-T_c|^{1/2}$ or $\propto |J-J_c|^{1/2}$).

Since the mean-field calculation overestimates critical temperatures, it is interesting to compare the previous results with the ones of another approximation (large N) that usually underestimates them. We have calculated the position of the PM-FM and PM-AFM phase transitions in the large-N approximation (see Appendix A):

$$\text{PM-FM line:} \quad T = +1.2578J + 0.5578,$$

$$\text{PM-AFM line:} \quad T = -1.2578J - 0.793. \quad (56)$$

The critical temperature is underestimated by roughly the same factor that the mean-field approximation overestimates it (see Fig. 1 of Ref. 4). To extend further this calculation would require a study of non-translationally-invariant saddle points, which is rather complex.

IV. MONTE CARLO SIMULATION

The model (1) can be investigated using a standard Monte Carlo method. We shall here describe some technical points, the results being discussed in the following subsections.

A single Monte Carlo (MC) step consists of a full-lattice Metropolis lattice sweep. Some of the simulations have been done at extremely low temperatures; thus the method of choice would have been a heat-bath algorithm, but its implementation in this model is rather complex. Fortunately, one can effectively falsify a heat-bath algorithm by means of a multihit Metropolis method, proposing per each hit as spin update a random spin on the unit sphere. Luckily enough, to achieve a 50% acceptance the number of needed hits is quite modest except for the lowest temperatures which represent a negligible fraction (below 1%) of the total CPU time devoted to the problem. The pseudo-random-number generator was

the congruential + Parisi-Rapuano (see, e.g., Ref. 34).

To extract critical exponents and critical temperatures, we have used the quotient methods:[18,19,35] for a pair of lattices of sizes L and $2L$ we choose the temperature where the correlation lengths in units of the lattice size coincide ($2\xi_L = \xi_{2L}$). Up to scaling corrections, the matching temperature is the critical point. Let now O be a generic observable diverging at the critical point like $|t|^{-x_O}$. Then, one has (up to scaling corrections[18,19,35])

$$\left.\frac{\langle O \rangle_{2L}}{\langle O \rangle_L}\right|_{\xi_{2L}/\xi_L=2} = 2^{x_O/\nu}, \quad (57)$$

where ν is the critical exponent for the correlation length itself. For extracting ν we have used the temperature derivative of the correlation length, $x_{\partial_T \xi} = 1 + \nu$. To satisfy the matching condition $2\xi_L = \xi_{2L}$ one often needs to extrapolate from the simulation temperature to a nearby one. This has been done using a reweighting method (see, e.g., Ref. 36).

A. Phase diagram

In previous work,[4] we studied in great detail the critical properties of the RP^2-PM phase transition at $J=-0.5$. The location of the critical lines was also reported. These critical temperatures were obtained via hysteresis cycles. We here report a finite-size scaling study of selected critical points in the phase diagram. Those points will be referred to as t_0 (FM-PM transition), t_1 (RP^2-AFI), t_2 (FM-FI), t_3 (AFM-AFI), and t_4 (RP^2-FI).

In all the five points t_0–t_4, we have simulated lattices L =6, 8, 12, 16, 24, 32, 48, and 64, producing 20×10^6 MC full-lattice sweeps for the largest lattices in each transition. We have discarded 5×10^5 MC steps for thermalization. In all cases this has been checked to be much larger than the integrated autocorrelation time. In addition, at the lowest temperatures, we have compared different starting configurations (random, FM, etc.), concluding that the results are start independent.

Before discussing the results let us briefly comment on what can be expected on universality grounds. Transition t_0 connects the paramagnetic phase, where the full O(3) symmetry group is preserved, to a FM phase where the symmetry group is just the O(2) group corresponding to the global rotations around the global magnetization. Thus it is expected (and confirmed) to be in the universality class of the O(3) nonlinear σ model (see Table III below). For all the other transitions the scheme of symmetry breaking is not so clear. The only obvious symmetry breaking (for transitions t_2 and t_3) is the symmetry between the even and odd sublattices. This is a Z_2 symmetry; thus one might expect the transition to be in the Ising universality class. The symmetries of the RP^2 phase are intriguing and will be investigated in the following subsection. Let us only recall that the transition between the PM and the RP^2 phase at $J=-0.5$ has been recently studied in great detail in Ref. 4. The critical exponent ν appears in Table III. Perhaps not unexpectedly, the critical exponents were found to be compatible within errors with that of the antiferromagnetic RP^2 model.[18,19]

TABLE I. J_c or T_c determined by the intersection of the correlation lengths measured in two lattices of size L and $2L$. $t_N(X,A)$ indicates the transition t_N, with X a fixed parameter and A the order parameter associated with the correlation length considered.

Transition	$L=6$	$L=8$	$L=12$	$L=16$	$L=24$	$L=32$
t_0 ($T=0.05, \mu^V$)	−0.453561(15)	−0.453293(32)	−0.453131(19)	−0.453090(15)	−0.453091(29)	
t_1 ($T=0.05, \mu^V$)	−0.59828(8)	−0.59939(4)	−0.60015(2)	−0.60038(1)	−0.60043(2)	−0.60044(2)
t_1 ($T=0.05, \mu_s^V$)	−0.60083(4)	−0.60084(3)	−0.60078(2)	−0.60067(1)	−0.60052(2)	−0.60048(2)
t_2 ($J=-0.43, \mu_s^V$)	0.017663(12)	0.017343(5)	0.017163(4)	0.017129(2)	0.017112(2)	0.017101(4)
t_3 ($J=-0.8, \mu^V$)	0.07528(4)	0.07387(2)	0.07304(2)	0.07283(1)	0.07267(1)	0.07260(1)
t_4 ($T=0.01, \mu^V$)	−0.47199(3)	−0.47198(2)	−0.47196(2)	−0.47195(1)	−0.471919(6)	−0.471916(3)
t_4 ($T=0.01, \mu_s^V$)	−0.47241(3)	−0.47219(3)	−0.47201(2)	−0.47196(1)	−0.471914(6)	−0.471912(3)

As for transitions t_0–t_4, we have located quite accurately the critical parameters (see Table I). We have focused in each case on the largest order parameter [see Eq. (22)]. The PM-AFM transition should have the same critical behavior and we have not invested computer time in this study. We are reasonably confident in the continuous nature of all five transitions. This stems from two facts. First, the energy histograms are not double peaked (see an example in Fig. 3). Yet, a much more refined test comes from the (L-dependent) value of the effective ν exponents shown in Table II. With the exception of transition t_0, which as expected belongs to the universality class of the Heisenberg model in three dimensions, scaling corrections are not even monotonic in their evolution with the lattice size. Although an asymptotic value cannot be guessed with reachable lattice sizes, at least one sees that, for the largest lattices, the exponent ν is reasonably far from the value $1/2$ to be expected in weak first-order transitions.

B. The RP² phase beyond mean field

As we have seen in Eq. (8), the effective Hamiltonian for the RP² phase is that of an RP² model. The neglected terms in Eq. (8) have lower symmetries and they could change this picture, but we shall see in Sec. IV C that this seems not to happen. To lighten the forthcoming discussion, we shall briefly recall here what it is known about the pure antiferromagnetic RP² model,[19] whose Hamiltonian is

$$H^{\mathrm{RP}^2} = \sum_{\langle i,j \rangle} (\vec{\phi}_i \cdot \vec{\phi}_j)^2. \tag{58}$$

The most striking feature of Eq. (58) is that it remains invariant under the transformation

$$\vec{\phi}_i \rightarrow -\vec{\phi}_i. \tag{59}$$

In other words, every spin can be reversed independently of the others. This symmetry is a local one, and the Elitzur theorem[22] tell us that it cannot be spontaneously broken. Therefore the spin-spin correlation function for the model (58) is

$$\langle \vec{\phi}_i \cdot \vec{\phi}_j \rangle = \delta_{ij}. \tag{60}$$

This means that the propagator (27) will be precisely $1/V$ for every p in the Brillouin zone. Of course the local symmetry (59) is at most approximated for the original Hamiltonian (1) if we are away from $T=0$ and $J=-0.5$. Yet we shall show
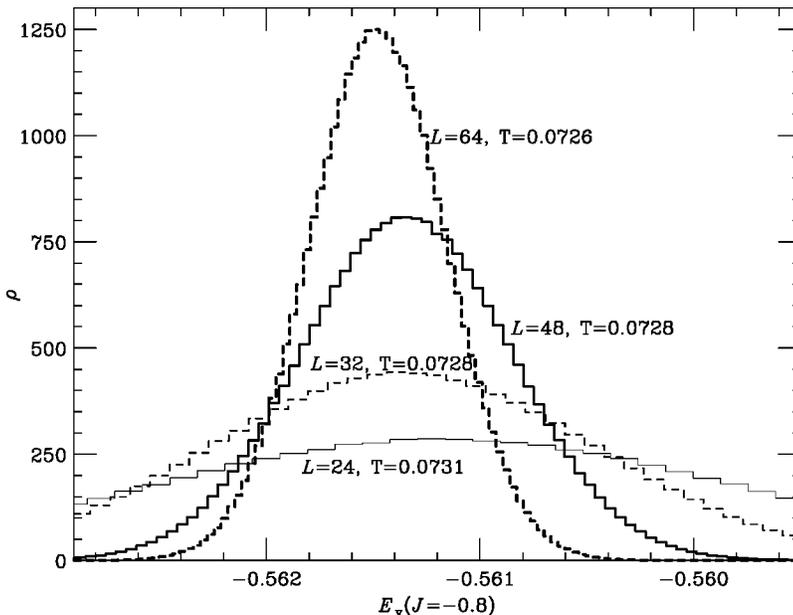

FIG. 3. Histogram for $E_v = \langle \vec{\phi}_i \cdot \vec{\phi}_j \rangle$ (for nearest neighbors i and j), in transition t_3.

TABLE II. Apparent ν exponent obtained from the quotient method applied to $(L, 2L)$ pairs.

Transition	$L=6$	$L=8$	$L=12$	$L=16$	$L=24$	$L=32$
t_0 $(T=0.05, \mu^{\mathrm{V}})$	0.707(4)	0.702(7)	0.712(12)	0.710(10)	0.629(95)	
t_1 $(T=0.05, \mu^{\mathrm{V}})$	0.594(20)	0.556(7)	0.555(8)	0.540(8)	0.546(17)	0.596(25)
t_1 $(T=0.05, \mu_{\mathrm{s}}^{\mathrm{V}})$	0.592(5)	0.561(6)	0.538(5)	0.519(7)	0.517(13)	0.561(22)
t_2 $(J=-0.43, \mu_{\mathrm{s}}^{\mathrm{V}})$	0.591(8)	0.569(5)	0.537(3)	0.548(5)	0.588(8)	0.604(17)
t_3 $(J=-0.8, \mu^{\mathrm{V}})$	0.583(10)	0.557(4)	0.562(3)	0.582(6)	0.605(7)	0.651(20)
t_4 $(T=0.01, \mu^{\mathrm{V}})$	0.534(4)	0.536(10)	0.560(10)	0.597(15)	0.630(17)	0.656(24)
t_4 $(T=0.01, \mu_{\mathrm{s}}^{\mathrm{V}})$	0.545(7)	0.564(13)	0.581(13)	0.611(16)	0.629(17)	0.650(25)

that the propagator is still of order $1/V$ in the full Brillouin zone, at a finite distance from $T=0$ and $J=-0.5$, for our model (see Fig. 5 below). Hence, if one considers the spins as *arrows*, there is no hint of any ordering in this region.

On the other hand, we shall show that the tensor correlation function (see also Ref. 19)

$$\langle (\vec{\phi}_i \cdot \vec{\phi}_j)^2 \rangle - \frac{1}{3} \qquad (61)$$

does not tend to zero at infinite distance. Hence, if one think of the spins as *segments* (that is, if one forgets about their sign), a global magnetic ordering exists.

As the reader can see, the ground state for the Hamiltonian (58) is very peculiar. The only constraint is that every spin must be orthogonal to its nearest neighbors. One may think about two extremal situations.

(1) One may put every single *even* spin aligned (or antialigned) with the (say) Z axis, while the spins on the odd sublattice are placed on the XY plane at *random*. On the whole, this ground-state is O(2) symmetric, as one can make a global rotation around the Z axis without changing the correlation functions. Notice, however, that the even and the odd sublattices play a very asymmetrical role. Yet, in the Hamiltonian (1), the two sublattices are equivalent. Hence, in this ground state we have a breaking of the O(3) symmetry

TABLE III. Critical exponent ν for some three-dimensional universality classes.

Model	ν
O(1) (Ising) (Ref. 37)	0.6294(10)
O(2) (Ref. 38)	0.67155(27)
O(3) (Ref. 39)	0.710(2)
O(4) (Ref. 39)	0.749(2)
O(5) (Ref. 40)	0.766
RP^2-AFM (Ref. 19)	0.783(11)
RP^2-PM (double exchange) (Ref. 4)	0.781(18)
Chiral (Heisenberg) (Ref. 30)	0.57(3)
Chiral (XY) (Ref. 30)	0.55(3)
Tricritical (Ref. 5)	$1/2$
Weak first order (Ref. 41)	$1/2$
First order	$1/3$

group to an O(2) subgroup, *and* a breaking of the even-odd symmetry. The translational invariance is reduced to the displacements that do not change the parity of the site.

(2) One may consider spins in the even sublattice aligned (or antialigned) with the (say) Z axis, while the spins on the odd sublattice are aligned (antialigned) with the (say) X axis. This ground state fully breaks the O(3) symmetry. Yet, the two sublattice play a symmetrical role. If one considers rotationally invariant correlation functions [such as $\langle (\vec{\phi}_i \cdot \vec{\phi}_j)^2 \rangle$ for any i and j], the translation group is not broken.

At first sight one could say that the first ground state has a much larger entropy. However, for the the second ground state, fluctuations for the even sublattice can be much larger than for the first ground state. To decide which ground state is realized, one may try a "spin-wave" calculation for each case (see Appendix C). At the leading order in the temperature one finds that their contribution to the partition function has the same power of T and consequently it is not straightforward to conclude analytically which is the stable phase.

A detailed numerical study[19] showed that at very low temperature the O(2)-symmetric ground state prevails. Yet, upon increasing the temperature, the correlations for the spins on the planar sublattice grow. The increased fluctuations of the collinear sublattice induce a ferromagnetic effective short-range coupling for the planar sublattice (*order from disorder*). One may wonder if this effective coupling (which grows with temperature) will be enough to break the remaining O(2) symmetry, before reaching the paramagnetic phase. The answer is negative. In Sec. IV C, we shall show that in the present model there is only a low-temperature phase, with a remaining O(2) symmetry, and where the even-odd symmetry is fully broken (see Fig. 7 below).

In the Introduction, we recalled the nonlinear σ model (NLσM) arguments[27] suggesting that this symmetry-breaking pattern implies that the universality class is the one of the O(3) NLσM. The numerical result—see Table III—seem hardly compatible with this possibility. Yet, one can produce an argument, suggesting a different conclusion.

If one wants to construct the Landau free-energy functional, in principle the two order parameters $\mathcal{M}$ and $\mathcal{M}_{\mathrm{s}}$ would appear. Yet the mean-field calculation (see also the Appendix in Ref. 19) has taught us that $\mathcal{M}$ is just the square of $\mathcal{M}_{\mathrm{s}}$. Thus, only $\mathcal{M}_{\mathrm{s}}$ appears in the functional. Notice $\mathcal{M}_{\mathrm{s}}$ transforms under the even-odd symmetry as $\mathcal{M}_{\mathrm{s}} \rightarrow -\mathcal{M}_{\mathrm{s}}$; hence only even powers of $\mathcal{M}_{\mathrm{s}}$ are present. Then, the more general form for the Landau potential (up to fourth order),
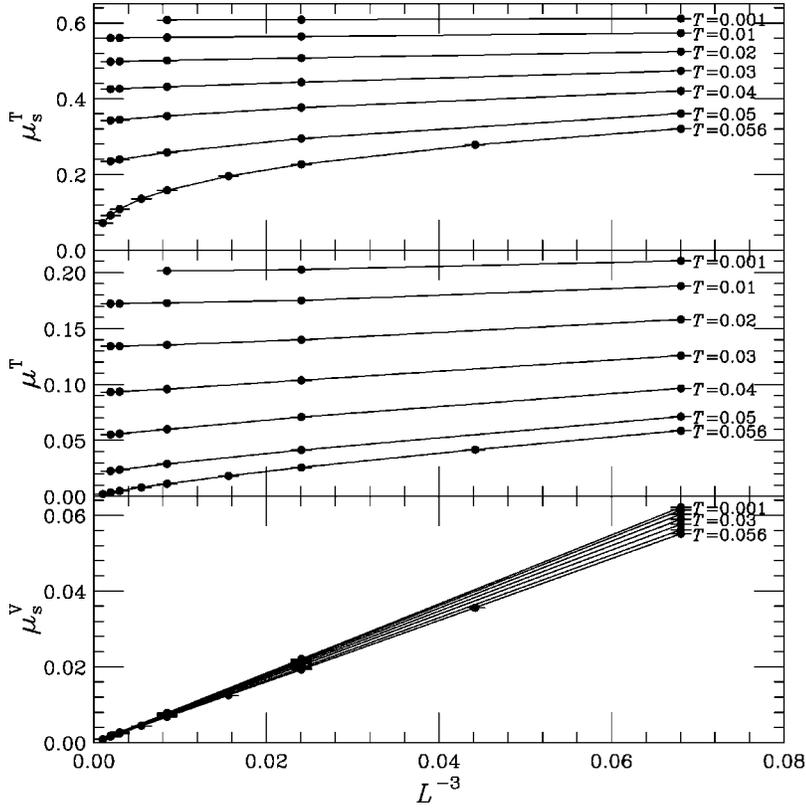
FIG. 4. Lattice size dependence of μ_s^T, μT, and μ_s^V at different temperatures, for $J=-0.5$.

compatible with the rotational symmetry of the Hamiltonian (1) is

$$U(\mathcal{M}_s) = \int d\mathbf{r}[g_2 \mathrm{Tr} \, \mathsf{M}_s^2 + g_4 (\mathrm{Tr} \, \mathsf{M}_s^2)^2 + g_4' \mathrm{Tr} \, \mathsf{M}_s^4]. \quad (62)$$

Now, the only constraint on $\mathcal{M}_s$ is that it is a symmetric traceless matrix:

$$\mathcal{M}_s = \begin{pmatrix} a & c & d \\ c & b & e \\ d & e & -a-b \end{pmatrix}. \quad (63)$$

If one introduces a five-component vector field

$$\Phi = \left(\frac{a+b}{\sqrt{2}}, \frac{a-b}{\sqrt{2}}, c, d, e \right), \quad (64)$$

it is easy to show that

$$\mathrm{Tr} \, \mathsf{M}_s^2 = 2(\Phi \cdot \Phi), \quad (65)$$

$$\mathrm{Tr} \, \mathsf{M}_s^4 = 2(\Phi \cdot \Phi)^2. \quad (66)$$

Thus, the Landau free-energy functional is identical to the one of an O(5) NLσM. And the numerical results (Table III) are in much better agreement with this possibility than with that of the O(3) NLσM.

C. Detailed study of the RP^2 phase

The RP^2 phase of model (1)—we do *not* refer to the ideal case of Eq. (58)—poses several questions: (1) Is the RP^2 phase truly segmentlike? [recall that the Hamiltonian (1) is not invariant under individual spin reversal]. (2) Is the even-odd symmetry broken up to the temperature separating the RP^2 phase from the paramagnetic state? (3) Is the low-temperature O(2)-symmetric RP^2 phase preserved up to the temperature separating the RP^2 phase from the paramagnetic state? We shall address them separately, in the stated order.

1. Tensor versus vector ordering

We have called RP^2 the phase in which the vector magnetization vanishes (for any momentum in the Brillouin zone), and the tensor magnetization is nonvanishing, both at momentum $(0,0,0)$ (μ^T) and at momentum (π, π, π) (μ_s^T). In Fig. 4 (top and middle parts) we show, fixing $J=-0.5$, that, for temperatures ranging from 0.001 to 0.05, there is a non-vanishing thermodynamic limit for both quantities. For comparison, we show in the bottom part the vector magnetization at momentum (π, π, π) (μ_s^V), which goes to zero as $1/\sqrt{L^3}$. We have also measured the correlation length in the vector channel. Although some short-range ordering is present, the correlation length is not larger than 0.3 lattice spacing.

To confirm the absence of any other vectorial magnetization we have measured at $J=-0.55$, $T=0.5$ (just in the middle of the RP^2 phase) all Fourier components of the vector field $\vec{\phi}_i$ for 90 statistically independent configurations for each lattice size, and plotted in Fig. 5 the corresponding momentum versus the maximum value of the Fourier component squared. In other words, we are searching for the maximum (over the Brillouin zone) of the static structure factor (divided by L^3). We have chosen as lattice sizes $L=6$, 8, 12, 30, 60 to allow for different periodicities of the
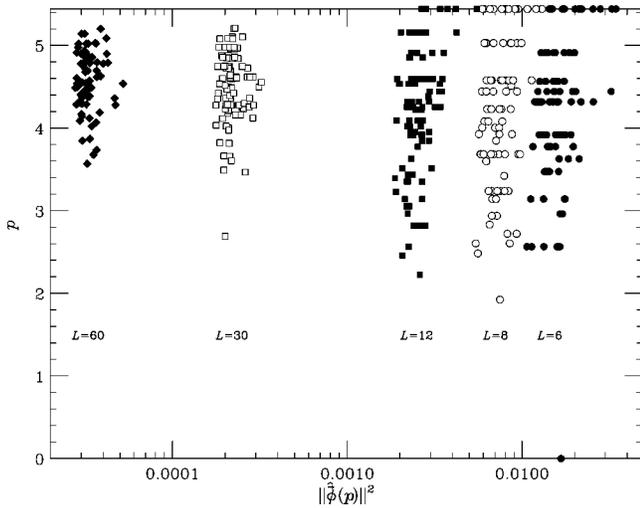
FIG. 5. Scatter plot for 90 statistically independent configurations for each lattice size ($L=6, 8, 12, 30, 60$) at $J=-0.55$, $T=0.5$. On the horizontal axis we plot the maximum over the Brillouin zone of the squared Fourier transform of the spin field, and on the vertical axis the corresponding associated momentum $p=\|\mathbf{p}\|$. The horizontal position of the legends scales as $L^{-3}\log L$ in agreement with the absence-of-order prediction.

would-be vector-ordered states. If no vectorial ordering is present, the last quantity should go to zero as $1/L^3$, up to logarithmic corrections that arise from the fact that we are computing the maximum of a set of $O(L^3)$ elements. The absence of ordering is clear from Fig. 5.

2. Even-odd symmetry

To analyze the even-odd symmetry, we measure the tensor correlation difference at second neighbors between even and odd lattices. The normalized total difference for a given configuration can be written as

$$\Delta_E = \frac{2}{3L^3}\left(\sum_{\text{even}}(\phi_i \cdot \phi_j)^2 - \sum_{\text{odd}}(\phi_i \cdot \phi_j)^2\right), \qquad (67)$$

where the sums extend over even (odd) second-neighbor pairs. The nonvanishing of the difference in the thermodynamic limit signals even-odd symmetry breaking. Notice that the sublattice energy difference can be defined locally, and it plays the role of a local field. Another interesting observable is the dimensionless quantity associated with the energy difference,

$$\kappa_E = \frac{\langle \Delta_E^2 \rangle}{\langle \Delta_E \rangle^2}. \qquad (68)$$

Figure 6 shows the tensor energy difference as a function of temperature for several lattice sizes. A clear nonvanishing thermodynamic limit for Δ_E is observed for $T<0.05$; therefore, the even-odd symmetry is broken up to this temperature. At $T=0.05$ the asymptotic behavior can be elucidated by a direct study of the tensor energy difference histograms. A $L=96$ lattice is necessary to clearly resolve the two-peak structure of the histogram (see Fig. 7), corresponding to an
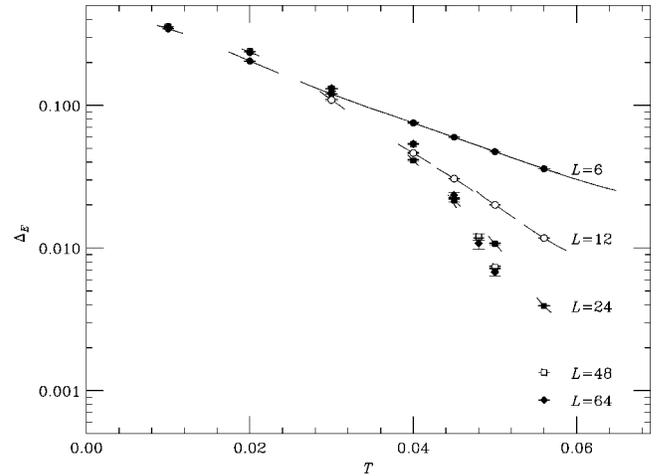

FIG. 6. Difference of the tensor second neighbors energies between sublattices, for $T=0.05$.

even-odd symmetry breaking. Notice that $L=96$ is the largest lattice used, which makes it impossible to study the thermodynamic limit of that quantity for T larger than 0.05 and less than $T_c=0.0559$. We can conclude that, within the computational resources employed, no evidence exists for a thermodynamic limit with unbroken even-odd symmetry.

Although no thermodynamic limit can be reached beyond $T=0.05$, more information can be obtained through a finite-size analysis. The closer we get to $T=0.05$, the harder it becomes to find a two-peak structure in the histogram. A correlation length could be defined in the even-odd symmetry breaking channel which grows as the possible critical point between the RP^2 phase with broken even-odd symmetry and a hypothetical RP^2 phase with restored even-odd symmetry is approached. The functional form of the growth of the correlation length might give an indication of the existence of such phase transition. A direct way to carry out that study is to define the correlation length as the lattice size itself, when the histogram has a central valley at half the peak hight. The result shows a growth of the correlation length as T increases compatible with a divergence just at T_c,
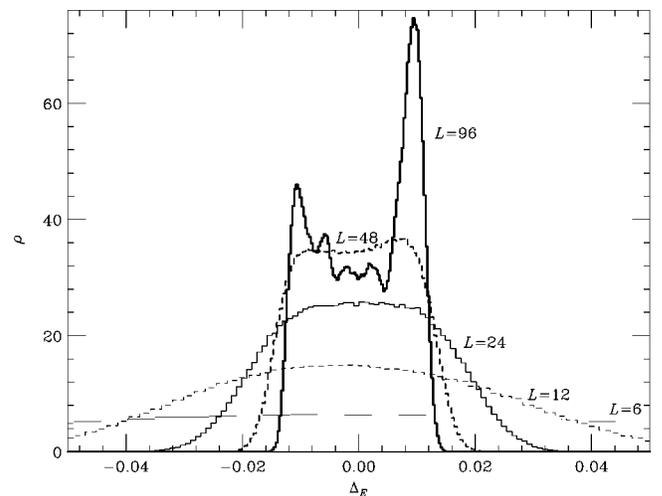

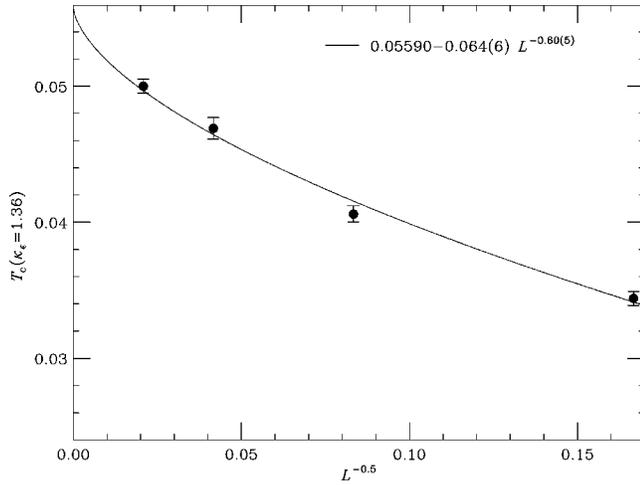FIG. 7. Histogram of Δ_E for $J=0.5$, $T=0.05$.

FIG. 8. Displacement of the critical temperature, defined as the point where κ_E takes a fixed value, as a function of size. Fits suggest that there is no even-odd symmetry restoration at a temperature less than the RP^2-PM one.

though with rather peculiar exponents. But the measurement of that correlation length is very noisy. A much more precise way to study the possible presence of a transition previous to T_c is to define as apparent critical point the T value at which κ_E takes a fixed value. Figure 8 shows the results. Although the possibility of an even-odd symmetry recovery transition previous to T_c cannot be discarded, results are compatible

with a divergence just at T_c. The figures show a fit to a power law (fixing the critical point to the value $T_c = 0.055\,895(5)$ obtained in Ref. 4). It is worth remarking that the effective ν exponent obtained with a power law fit is very large (2 or larger), which might point to a logarithmic divergence. Thus, all our results point to a single RP^2 phase with broken even-odd symmetries at all temperatures.

3. O(2) symmetry

The chosen tool to study whether the O(2) symmetry of the $T=0$ state is preserved at higher temperatures has been the eigenvalue structure of the tensor $\mathcal{M}_s$. The latter being traceless implies that the vector $\boldsymbol{\lambda}=(\lambda_1,\lambda_2,\lambda_3)$ must lie on the $x+y+z=0$ plane. The whole information reduces, then, to a modulus (which is nothing but the observable μ_s), and an angle, which contains all the information of the eigenvalues on the symmetry O(2). As any result must be symmetric under eigenvalue permutations and global inversion, we can restrict the angle to the interval between 0 and $\pi/6$. More precisely, we consider the orthonormal basis $\{\mathbf{u}_x,\mathbf{u}_y\}$ for the plane given by

$$\mathbf{u}_x = \frac{1}{\sqrt{2}}(-1,1,0), \tag{69}$$

$$\mathbf{u}_y = \frac{1}{\sqrt{6}}(-1,-1,2). \tag{70}$$

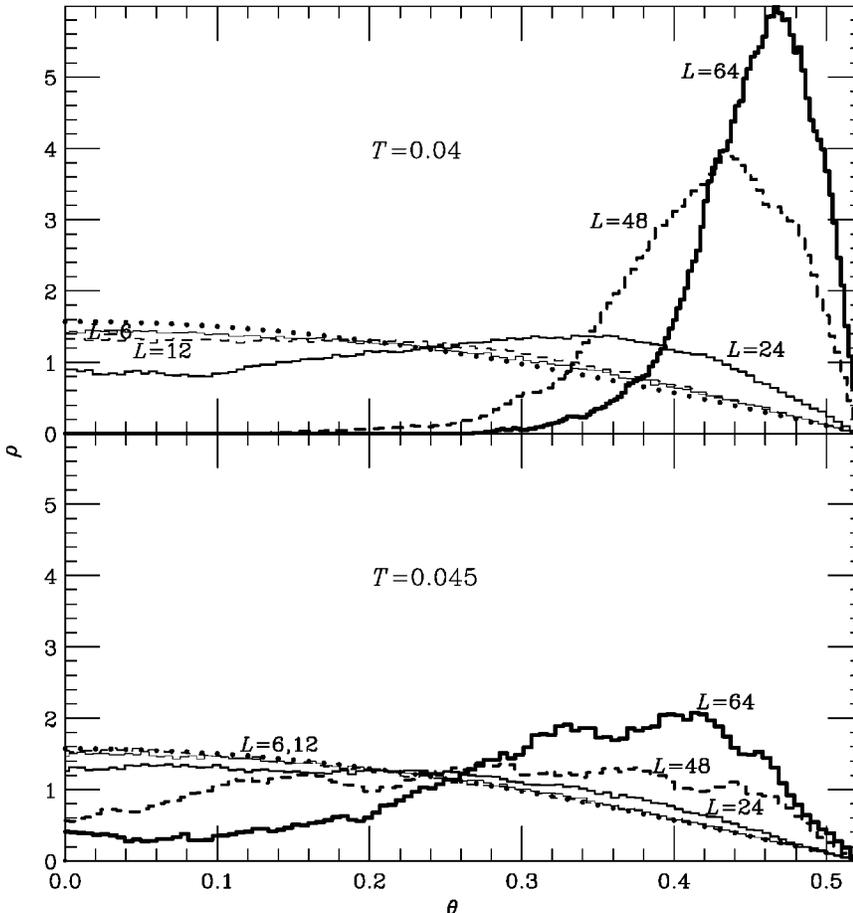and define the angle θ from the relation

FIG. 9. Histograms of the angle of the eigenvalue vector on the $(1,1,1)$ plane for two temperatures at $J=-0.5$. The dots correspond to paramagnetic configurations.
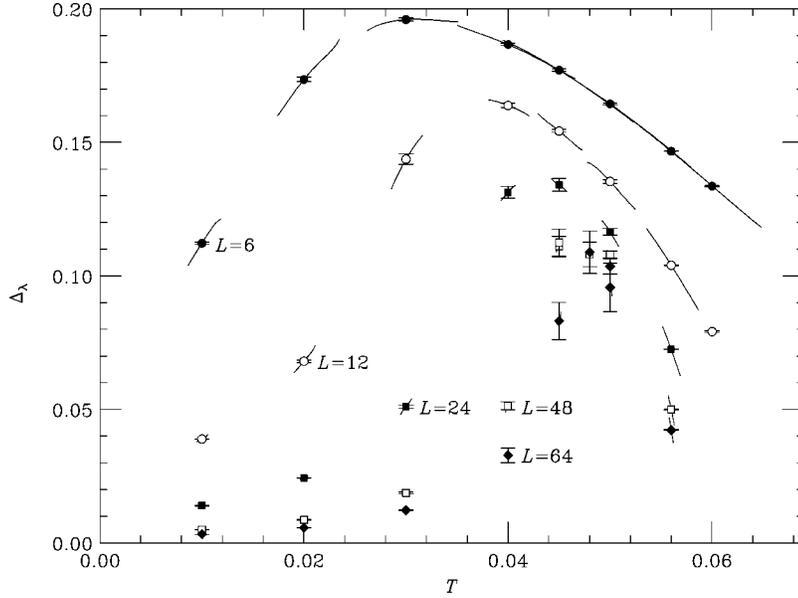
FIG. 10. Modulus of the difference between the two smaller eigenvalues of $\mathcal{M}_s$ as a function of T.

$$\tan\theta = \frac{\boldsymbol{\lambda} \cdot \mathbf{u}_y}{\boldsymbol{\lambda} \cdot \mathbf{u}_x}, \tag{71}$$

with the proviso that we choose a permutation and a global sign such that θ lies between 0 and $\pi/6$.

Another interesting quantity can be defined as follows. In the thermodynamic limit an O(2)-symmetric phase corresponds to $\lambda_2 = \lambda_3$. We thus define

$$\Delta_\lambda = |\lambda_2 - \lambda_3|, \tag{72}$$

which must vanish in the thermodynamic limit if the O(2) symmetry is not broken. As usual the corresponding dimensionless quantity is

$$\kappa_\lambda = \frac{\langle \Delta_\lambda^2 \rangle}{\langle \Delta_\lambda \rangle^2}. \tag{73}$$

Figure 9 shows histograms of angles at several temperatures and lattice sizes. Dotted lines correspond to completely disordered configurations. In case of the system being O(2) symmetric (one large eigenvalue and two identical small eigenvalues), the distribution should be a δ function at angle $\pi/6$. For a system with broken O(2) symmetry but unbroken even-odd symmetry, the eigenvalues are $(a, 0, -a)$-like, which would correspond to a Dirac δ function at angle 0. We notice that, for small lattices, the distribution points to complete disorder, but as the size grows an inflection point turns up at $T = 0.04$, 0.045 for $L = 24$, 48, respectively, and as L goes on growing a peak arises at angles ever closer to the maximum. It might be said that the behavior in L is always the same, except for a scale change.

Another interesting quantity is the difference between the two small eigenvalues (Δ_λ), which should vanish in the presence of O(2) symmetry, so turning out to be an order parameter. Figure 10 shows that quantity for several values of the temperature and lattice size. If we look at an intermediate size ($L = 24$, for instance) the appearance is that of a transi-

tion at $T = 0.03$ to a phase with broken O(2) symmetry. Yet, as L increases, the apparent transition moves back, approaching T_c ever more closely.

To check the consistency of the results with respect to the existence of a transition within the RP^2 phase we can perform a finite-size scaling study fitting $\Delta_\lambda L^{\beta/\nu}$ as a function of $(T - T_0)L^{1/\nu}$. Only $T_0 = T_c$ yields a reasonable fit (see Fig. 11). Notice that for T close to T_c the definition of Δ_λ ceases to be meaningful, as a large eigenvalue exists no longer since the RP^2 magnetization fades away, and no good fit can be expected. However, for most T values (more precisely, for $T < 0.05$) the fit is excellent, though the η and ν values are admittedly rather unusual ($\eta = -0.5$, $\nu = 1.8$). The conclusion should be that there is no evidence for an O(2)-breaking transition at any finite distance from T_c. A collapse of that transition over the RP^2-PM transition might occur.

A more quantitative analysis can be made studying the displacement of the temperature at a fixed value of κ_λ. In Fig. 12 we plot the obtained measures together with fits to several functional forms: a power law with the critical temperature fixed to $T_c = 0.055\,895(5)$,[4] a three-parameter power law, and a Kosterlitz-Thouless-like divergence. The results point again to no breaking of the O(2) symmetry inside the RP^2 phase.

D. Interplay between ferromagnetism, antiferromagnetism, temperature, and an applied magnetic field in the low-doped La$_{1-x}$Sr$_x$MnO$_3$

In a series of papers[23–26] the interplay between FM, AFM, temperature, and an applied magnetic field in the low-doped La$_{1-x}$Sr$_x$MnO$_3$, mainly at x close to 1/8, has been studied. We would like to point out some properties of our FM-FI phase transition (point t_2 in this paper) which might help to understand phenomena which, in those references, are related to the FM-CO (charge ordered) phase transition, not fully understood so far.

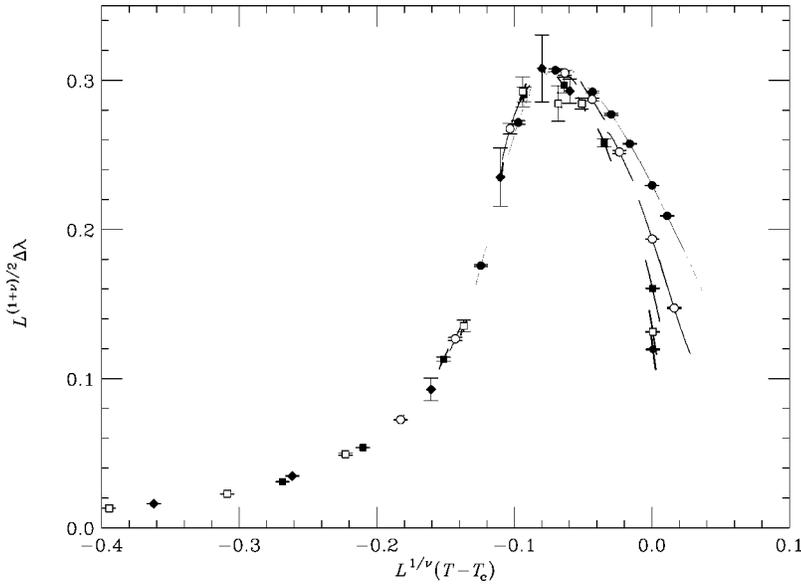Roughly speaking, some of the mentioned phenomena are as follows.

FIG. 11. Scaling of Δ_λ for the analysis of a possible O(2) restoring transition. Data are fairly well fitted assuming the transition occurs at T_c (points next to T_c are not well fitted because there the largest eigenvalue becomes zero and Δ_λ ceases to make sense). The fitted values are $\eta=-0.5$, $\nu=1.8$, $T_c=0.0559$.

(1) Resistance increases as T decreases below T_{CO} (t_2 in our model). In our simplified model, this corresponds to the fact that, when crossing the FM-FI transition, odd and even spins cease to be aligned, which makes conductivity via DE harder.

(2) Experimentally,[23] the charge-ordered phase grows larger when an external magnetic field is applied. In our case, we have run a simulation with nonzero magnetic field and, as pointed out in italics in the second next paragraph, our FI phase invades the FM phase and the critical temperature rises.

(3) In the CO phase, at fixed temperature, the magnetization increases with an external magnetic field, just as in a FM phase.

Let us now describe the physics of the FM-FI transition. Near the FM-FI transition, in the FM phase the ordering is symmetric with respect to the odd-even exchange and the field fluctuates at random around the total magnetization vec-

tor, the fluctuations being larger than in the FI phase, as shown by measurements of specific heats and susceptibilities made in both phases. More precisely, the magnetization increases as the temperature goes down from the FM to the FI phase, which can be explained by a diminution of fluctuations. In fact, one would expect that the magnetization should be smaller in the FI phase, with fixed odds and evens on an open cone around the odd direction, than in the FM phase, where the evens lie on a narrower cone, with a larger projection on the odd direction. Yet, the large fluctuations in the FM phase destroy the even contribution to the magnetization. The FI vacuum consists then of the odd, practically frozen, sublattice, and the even sublattice, with spins on an open, but less fluctuating cone.

Let us now look at the FM phase close to the FI transition, and switch on a weak magnetic field in the Z direction. This will have the general effect of collimating the spins. In more detail, odd spins will freeze closer to the Z direction, which
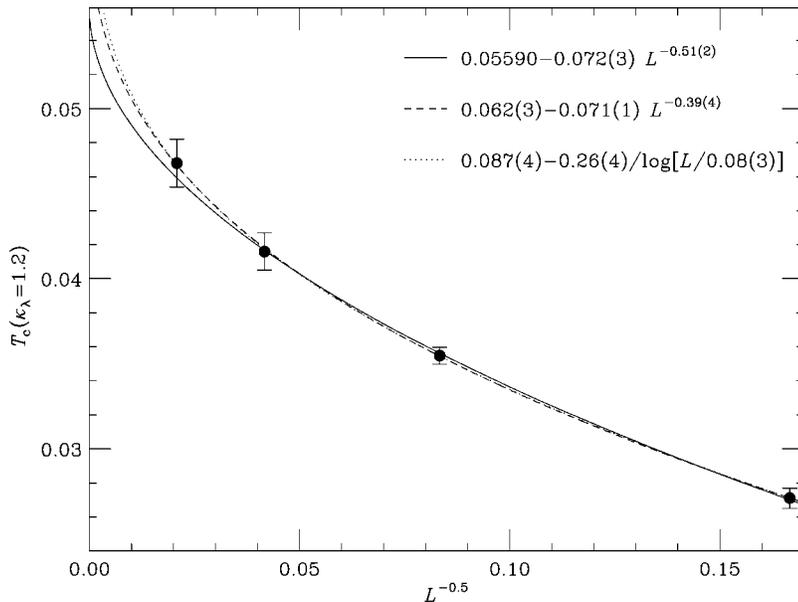

FIG. 12. Displacement of the critical temperature, defined as the point where κ_λ takes a fixed value, as a function of size. Fits suggest that there is no O(2)-breaking transition, at a temperature less than the RP^2-PM transition temperature.
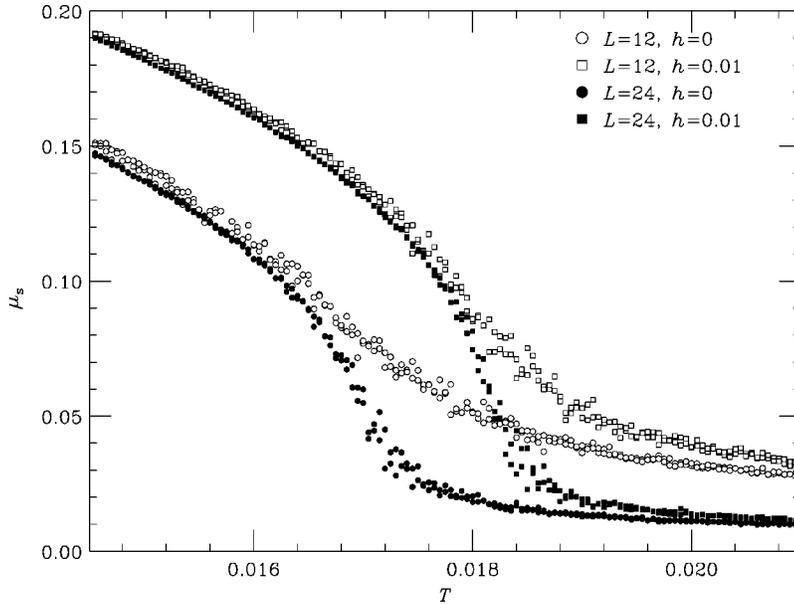
FIG. 13. Hysteresis along t_2. The transition occurs in the region where μ_s^V changes suddenly, and the figure shows a movement of T_c to higher values when $h=0.01$ is switched on $[T_c(h=0) =0.0171]$.

will cause the even sublattice to freeze on the cone, with smaller fluctuations. Paradoxically, the collimating effect of the magnetic field in the Z direction is to stabilize the cone, effectively opening it, giving rise to a more FI-like ordering, i.e., *the FI phase invades the FM phase, and the critical temperature rises*. This phenomenon (see point 2) is accompanied by an increase in the magnetization at fixed temperature in the FI phase (see point 3).

In order to check the correctness of the description, we have simulated in the neighborhood of the transition with $h=0.01$, which does not alter the system properties, and have run a hysteresis cycle at $J=-0.43$ in $L=12$, 24 between $T=0.01$ and $T=0.025$ (i.e., along t_2). A good observable for the transition is μ_s^V. The results at the two L values show that the finite-size effects are negligible compared with the change in T_c with h.

Figure 13 shows the result, which confirms that the inclusion of a magnetic field rises T_c, causing the invasion of the FI ordering into regions which at $h=0$ were FM.

V. CONCLUSIONS

We have studied a simple model for double-exchange interactions which retains a good number of interesting properties. It exhibits a complex phase diagram with ferromagnetic and ferrimagnetic phases, with their staggered counterparts, and a segment-ordered phase.

We obtain quantitatively all phases with approximate calculations (mean field and $1/N$ expansions), which can be contrasted with *exact* Monte Carlo calculations. The mean-field calculation is also useful to formulate a Ginzburg-Landau functional for the RP^2 phase.

With Monte Carlo simulations we obtain, in addition to the precise positions of the transitions, information about their order. Our conclusion is that all transitions seem to be second order, although an accurate determination of the critical exponents is difficult and it is beyond the scope of this paper.

We have studied in detail the *exotic* RP^2 phase (segment ordered), concluding that it is a single phase up to the resolution allowed by the lattice sizes used in the simulation. The presence of a RP^2 phase up to $T=0$ is interesting from the experimental point of view, since it can be confused with a PM or glassy phase and consequently with a quantum critical point. We have shown that the structure factor $(L^3\|\hat{\vec{\phi}}(\boldsymbol{p})\|$, in Fig. 5) remains bounded in the full Brillouin zone. Therefore the RP^2 phase cannot be detected in neutron-scattering experiments as a long-range ordering, although the phase transition will show up as a maximum (more precisely, a cusp) of the specific heat. A short-range ordering would of course always be present. Since the critical exponent α is negative, the Harris criterion[42] implies that our results are robust against disorder effects. The RP^2 phase is characterized by a breakdown of the even-odd symmetry and a remaining O(2) symmetry. A $2+\epsilon$ expansion[27] suggests that the critical exponents must be those of the classical Heisenberg model. Yet, if one constructs a Ginzburg-Landau functional, the natural conclusion is that the universality class is the one of the O(5) nonlinear σ model. This last possibility seems to be the one realized in practice.

We have also discussed the effects of a magnetic field on the ferromagnetic-ferrimagnetic transition, and we have discussed its interplay with electrical conductivity.

APPENDIX A: LARGE-*N* APPROXIMATION

We write the model as

$$\mathcal{H} = -N\sum_{\langle i,j\rangle} W(1 + \vec{\phi}_i \cdot \vec{\phi}_j). \tag{A1}$$

The Boltzmann weight is $\exp(-\mathcal{H})$ and

$$W(x) = Jx + \sqrt{x}. \tag{A2}$$

Using the expression of the Dirac δ functions (one to fix the spin modulus $\vec{\phi}_i^2 = 1$ and another to write that $x = \vec{\phi}_i \cdot \vec{\phi}_j$) in terms of functional integrals, we can write the partition function of the model in the following way:[43,44]

$$Z \propto \int d[\rho,\lambda,\mu,\vec{\phi}]e^{NA}, \tag{A3}$$

with A, the action, as

$$A = \frac{\beta}{2}\sum_{\langle i,j\rangle} [\lambda_{ij} + \lambda_{ij}\vec{\phi}_i \cdot \vec{\phi}_j - \lambda_{ij}\rho_{ij} + 2W(\rho_{ij})]$$

$$-\frac{\beta}{2}\sum_i \mu_i(\vec{\phi}_i^2 - 1). \tag{A4}$$

As we are interested (in this part of the calculation) in paramagnetic or/and ferromagnetic phases, we separate the spin into two pieces: the first one parallel to the symmetry-breaking direction, $\phi^{\parallel}$ (one degree of freedom), and the orthogonal part ($N-1$ degrees of freedom), $\vec{\phi}^{\perp}$. At this point, the spins have no definite modulus, and we can perform the functional integration over the orthogonal part of the spins (a Gaussian integral)

$$\int d[\vec{\phi}^{\perp}]e^{-(1/2)\vec{\phi}^{\perp}\cdot\hat{R}\vec{\phi}^{\perp}} \propto \exp\left(-\frac{N-1}{2}\mathrm{Tr}\log\hat{R}\right), \tag{A5}$$

where R_{ij}^{ab} is the propagator ($a,b = 1,\ldots,N-1$ and i exists in the three-dimensional lattice) and is given by

$$R_{ij}^{ab} = \delta^{ab}\beta\left(\beta\mu_i\delta_{ij} - \frac{1}{2}\sum_{\nu}\lambda_{ij}\delta_{i_{\nu}j}\right). \tag{A6}$$

The sum runs back and forth along the three lattice axes and i_{ν} is the neighbor of site i in the direction defined by ν. The trace Tr is over the space and spin components. The quantity $\frac{1}{2}(\vec{\phi}^{\perp}\cdot\hat{R}\vec{\phi}^{\perp})$ is the contribution to A involving the orthogonal part of the spins (which is a quadratic form with matrix $\hat{R}$).

In momentum space, $\hat{R}$ reads

$$R^{ab}(\boldsymbol{q},\boldsymbol{q}') = \delta^{ab}\frac{\beta}{V}\sum_i e^{i(\boldsymbol{q}-\boldsymbol{q}')\cdot\boldsymbol{r}_i}$$

$$\times\left(\mu_i - \frac{1}{2}\sum_{\nu}[\lambda_{ii_{\nu}}e^{i\boldsymbol{q}'\cdot\boldsymbol{\nu}} + \lambda_{i_{-\nu}j}e^{-i\boldsymbol{q}'\cdot\boldsymbol{\nu}}]\right), \tag{A7}$$

where $\boldsymbol{\nu} = \boldsymbol{r}_{i_{\nu}} - \boldsymbol{r}_{\nu}$. In the large-*N* technique we must maximize A. In order to keep the computation at its simplest level, we make an ansatz over the fields λ_{ij}, μ_i, ρ_{ij}, and $\phi^{\parallel}$: we are assuming that we will describe under this ansatz translationally invariant phases, like paramagnetic and ferromagnetic ones. So we will consider that all these fields are independent of x and μ and we will write them as λ, ρ, μ, and σ. Therefore, A is

$$\frac{A}{V} = \frac{\beta}{2}d[\lambda(1-\rho) + \lambda\sigma^2 + 2W(\rho)]$$

$$+ \frac{\beta}{2}\mu(1-\sigma^2) - \frac{1}{2}\int dq\,\log\left[\mu - \lambda\sum_{\nu}\cos q_{\nu}\right], \tag{A8}$$

where d is the dimension of space and

$$\int dq \equiv \int_{[0,2\pi)^d}\frac{d^dq}{(2\pi)^d} = 1. \tag{A9}$$

Hence, this computation is valid in paramagnetic and ferromagnetic phases where we have translational invariance. As usual we write

$$\hat{p}^2 \equiv 4\sum_{\nu}\sin^2(p_{\nu}/2). \tag{A10}$$

The continuum limit of $\hat{p}^2$ is p^2, and so we can define a mass m_0:

$$m_0^2 = \frac{2\mu}{\lambda} - 2d \tag{A11}$$

and A can be written as

$$\frac{A}{V} = \frac{\beta}{2}d[\lambda(1-\rho) + \lambda\sigma^2 + 2W(\rho)] + \frac{\beta}{2}\mu(1-\sigma^2)$$

$$-\frac{1}{2}\log\lambda - \frac{1}{2}\int dq\,\log[m_0^2 + \hat{p}^2]. \tag{A12}$$

The saddle point equations are

$$\beta d(1-\rho) + \frac{1}{\lambda}[(m_0^2 + 2d)I(m_0^2) - 1] + d\beta\sigma^2 = 0, \tag{A13}$$

$$\beta(1-\sigma^2) = \frac{2}{\lambda}I(m_0^2), \tag{A14}$$

$$2W'(\rho) = \lambda, \tag{A15}$$

$$\sigma(d\lambda - \mu) = 0, \tag{A16}$$

where

$$I(m_0^2) \equiv \int dq\,\frac{1}{m_0^2 + \hat{p}^2}. \tag{A17}$$

One solution is $\sigma = 0$, the paramagnetic phase. We can find a second-order phase transition by fixing the mass m_0 to zero:

$$TI(0) = J + \frac{1}{2\sqrt{\rho_0}}, \tag{A18}$$

where

$$\rho_0 = 2 - \frac{1}{2dI(0)}. \tag{A19}$$

In three dimensions $I(0) \simeq 0.2527$. So we have found the critical line between the paramagnetic and ferromagnetic phases. This solution is only valid in $J > -1/2$. It is easy to check that the $J = -1/2$ vertical line corresponds to infinite mass. So, with these formulas we cannot reach the region to the left of $J = -1/2$. Below we will see how to solve this drawback.

We can try to connect this calculation with the $T = 0$ results. The solution $\sigma \neq 0$ implies that $d\lambda = \mu$ and so $m_0^2 = 0$. Notice that in a magnetized phase, m_0 has no longer the meaning of a mass (hence, in this case, $m_0 = 0$ is not a signature of criticality). In this case the complete solution is

$$\rho^* = 2 - \frac{1 - \sigma^2}{2I(0)d}, \tag{A20}$$

and

$$T = \frac{1 - \sigma^2}{I(0)}\left[J + \frac{1}{2\sqrt{\rho^*}} \right]. \tag{A21}$$

This last equation tells us what is the magnetization $1 - \sigma^2$ in a given point (T, J). In the interval $J > -1/2$ we obtain the solution $\sigma = 1$. In addition in the interval $J \in (-1/2, -1/(2\sqrt{2}))$ a second solution with $\sigma < 1$ appears. This is the signature of the ferrimagnetic phase. Hence, we have recovered part of the previous $T = 0$ results.

As mentioned, above the previous calculation is valid only in paramagnetic and ferromagnetic phases. In order to manage the paramagnetic and antiferromagnetic phases we use the following trick: we change the sign of the odd spins and we leave unchanged the even spins, so the Hamiltonian reads

$$\mathcal{H} = -N\beta \sum_{\langle i,j \rangle} W(1 - \vec{\phi}_x \cdot \vec{\phi}_y), \tag{A22}$$

and following the technique outlined above, we obtain the equations of the saddle point:

$$\lambda = -2W'(\rho), \tag{A23}$$

$$1 - \sigma^2 = \frac{2T}{\lambda}I(m_0^2), \tag{A24}$$

$$d\rho = d(1 - \sigma^2) - \frac{T}{\lambda}[(2d + m_0^2)I(0) - 1], \tag{A25}$$

$$\sigma(d\lambda - \mu) = 0. \tag{A26}$$

Again $m_0^2 = 2\mu/\lambda - 2d$.

In the paramagnetic phase $\sigma = 0$ is the solution and the equation of the critical line is (obtained by fixing $m_0^2 = 0$)

$$-TI(0) = J + \frac{1}{2\sqrt{\rho_0}}, \tag{A27}$$

where

$$\rho_0 = \frac{1}{2dI(0)}. \tag{A28}$$

In addition $0 < \sigma < 1$ is also a solution and so $d\lambda = \mu$ and this implies, as in the PM-FM computation, that $m_0^2 = 0$ The phase being a (staggered) magnetized one, this does not imply criticality. The solution is then

$$\rho^* = \frac{1 - \sigma^2}{2I(0)d} \tag{A29}$$

and

$$T = -\frac{1 - \sigma^2}{I(0)}\left[J + \frac{1}{2\sqrt{\rho^*}} \right]. \tag{A30}$$

As in the PM-FM case, this last equation tells us what is the magnetization $1 - \sigma^2$ in a given point (T, J). Again, in this part of the calculation we cannot reach the region $J > -1/2$. The line $J = -1/2$ has again $m_0^2 = 0$.

Finally, we report the transition lines in terms of the temperature measured in the Monte Carlo simulation. Taking into account that $T_{\mathrm{MC}} = T/N$, where T is the temperature of the large-N calculation, and fixing N to 3, we obtain the FM-PM line

$$T_{\mathrm{MC}} = 1.2578J + 0.5578, \tag{A31}$$

and the AFM-PM line

$$T_{\mathrm{MC}} = -1.2578J - 0.793. \tag{A32}$$

APPENDIX B: MEAN-FIELD FOURTH-ORDER ANALYSIS

We have extended our mean-field power expansion analysis to fourth order, so that we can find transitions where the paramagnetic phase is not involved. The analytical minimization with respect to all fields is a very hard task. But we can face the problem by restricting the parameter region, using the essential fields that can describe the transition. First of all, let us explore the transitions inside the ferromagnetic region found in the second-order analysis:

$$\Phi_{h\lambda_s}(\lambda_s) = \Phi(h^{\min}, 0, 0, \lambda_s), \tag{B1}$$

where $h^{\min}$ is the value of h where $\Phi_h(h) = \Phi(h, 0, 0, 0)$ reaches the minimum. We can expand

$$\Phi_{h\lambda_s}(\lambda_s) = \Phi(h^{\min}, 0, 0, 0) + a_{h\lambda_s}(T, J)\lambda_s^2 + b_{h\lambda_s}(T, J)\lambda_s^4 + O(\lambda_s^4). \tag{B2}$$

Then, if $b_{h\lambda_s}(T, J)$ is positive there is a stable minimum with nonzero λ_s when $a_{h\lambda_s}(T, J)$ is negative. Therefore, we find a transition line when $a_{h\lambda_s}(T, J) = 0$. In this case $b_{h\lambda_s}(T, J) > 0$ if $T < 0.31$ and the transition line between the ferromagnetic

and a ferrimagnetic phase, where M and M_s are nonzero, is

$$T_{\text{FM-FI}} = -\frac{4(20 + 83\sqrt{2}J + 140J^2)}{386\sqrt{2} + 875J + \sqrt{369\,392 + 971\,810\sqrt{2}J + 1\,265\,425J^2}}. \quad \text{(B3)}$$

We can do a similar analysis inside the RP^2 phase. In this case we study

$$\Phi_{\lambda_s h}(h) = \Phi(h, 0, 0, \lambda_s^{\min}), \quad \text{(B4)}$$

and

$$\Phi_{\lambda_s h_s}(h_s) = \Phi(0, h_s, 0, \lambda_s^{\min}), \quad \text{(B5)}$$

obtaining the following transition lines:

$$T_{\text{RP}^2\text{-FI}} = \frac{32(327 + 406\sqrt{2}J)}{35(480\sqrt{2} + 539J + \sqrt{-575\,136 - 768\,768\sqrt{2}J + 290\,521J^2})}, \quad \text{(B6)}$$

$$T_{\text{RP}^2\text{-AFI}} = \frac{32(283 + 406\sqrt{2}J)}{35(-128\sqrt{2} + 539J - \sqrt{929\,312 + 1148\,224\sqrt{2}J + 290\,521J^2})}. \quad \text{(B7)}$$

Finally, inside the antiferromagnetic phase we find a transition to an antiferrimagnetic ordering minimizing

$$\Phi_{h_s \lambda_s}(\lambda_s) = \Phi(0, h_s^{\min}, 0, \lambda_s). \quad \text{(B8)}$$

The transition line is

$$T_{\text{FM-FI}} = -\frac{4(404 + 795\sqrt{2}J + 700J^2)}{5(296\sqrt{2} + 875J + \sqrt{463\,688 + 1\,085\,630\sqrt{2}J + 1\,265\,425J^2})}. \quad \text{(B9)}$$

The fourth-order phase diagram is depicted in Fig. 14, together with the numerical calculation of Sec. III. Letting aside the FM-RP^2 line (which is first order in the mean-field approximation), the results of the fourth-order approximation are qualitatively satisfying.
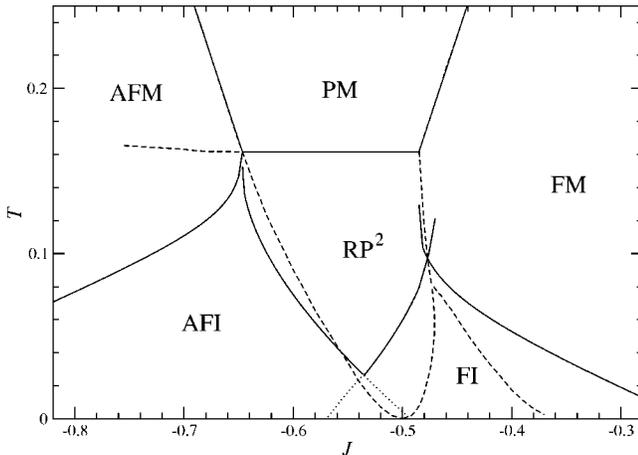

FIG. 14. Mean-field phase diagram as obtained from the numerical minimization of the free energy (dashed lines) and from the minimization of the free energy calculated to fourth order (full lines). The dotted lines are artifacts of the fourth-order approximation.

APPENDIX C: SPIN-WAVE CALCULATION

The aim of this appendix is to show that a straightforward spin-wave calculation for the very low temperature behavior of the RP^2 phase does *not* decide between the fully broken O(3) phase and an O(2)-symmetric one. For the sake of simplicity, we consider a simple antiferromagnetic RP^2 interaction $(\vec{\phi}_i \cdot \vec{\phi}_j)^2$.

1. O(2)-symmetric hypothesis

The vector sense does not play any role in the calculation of the free energy. In other words, we may change arbitrarily the sign of each spin independently of the others. Hence, we choose the sense of the spins on the even sublattice in such a way that they vary smoothly from site to site. We write the "even" field as

$$\vec{\phi}_{\text{even}} = \left(\sqrt{1 - v_y^2 - v_z^2}, v_y, v_z\right), \quad \text{(C1)}$$

where v_y and v_z are expected to be small (in absolute value) real numbers, that is, spin waves. The integration measure is then

$$\int_{S^2} D\vec{\phi}_{\text{even}} \approx 2 \int \int_{v_y^2 + v_z^2 \leqslant 1} \frac{dv_y dv_z}{\sqrt{1 - v_y^2 - v_z^2}}. \quad \text{(C2)}$$

The equality sign does not hold in the last expression, because we are integrating only over half the sphere (remember

that the spin waves are expected to be small).

On the other hand, the "odd" spins are parametrized as

$$\vec{\phi}_{\text{odd}} = \left(u_x, \sqrt{1 - u_x^2}\cos\varphi, \sqrt{1 - u_x^2}\sin\varphi\right), \qquad (C3)$$

the integration measure being

$$\int_{S^2} D\vec{\phi}_{\text{odd}} = \int_{-1}^{1} du_x \int_0^{2\pi} d\varphi. \qquad (C4)$$

In this case, only u_x is expected to be small (as the spins are basically restricted to be in the plane YZ). The fluctuations of the angles φ can be large.

The contribution of a pair of nearest neighbors to the action is

$$-\frac{1}{T}(\vec{\phi}_{\text{even}} \cdot \vec{\phi}_{\text{odd}})^2 = -\left[\tilde{u}_x\sqrt{1 - T(\tilde{v}_y^2}\right.$$
$$+ \tilde{v}_z^2) + \tilde{v}_y\sqrt{1 - T\tilde{u}_x^2}\cos\varphi$$
$$\left. + \tilde{v}_z\sqrt{1 - T\tilde{u}_x^2}\sin\varphi\right]^2, \qquad (C5)$$

where $\tilde{u}_x = u_x/\sqrt{T}, \tilde{v}_y = v_y/\sqrt{T}, \tilde{v}_z = v_z/\sqrt{T}$. Power expanding the RHS of Eq. (C5) at lowest order in T and the fields we obtain a temperature-independent contribution to the action:

$$(\text{RHS}) = -[\tilde{u}_x + \tilde{v}_y\cos\varphi + \tilde{v}_z\sin\varphi]^2 + \cdots. \qquad (C6)$$

The ellipsis stands for contributions vanishing for $T=0$. Yet, the change of variable from u_x, v_y, v_z to $\tilde{u}_x, \tilde{v}_y, \tilde{v}_z$ yields a factor T per each even site ($V/2$ factors), and a factor $\sqrt{T}$ per each odd site. Hence, the partition function, at the leading order in temperature, is

$$Z = T^{3V/4}(k^V + \cdots), \qquad (C7)$$

where k is a temperature-independent constant, and the ellipsis stands for subdominant terms at low temperature. Hence, the free-energy density varies as

$$f \sim -\frac{3}{4}T\log T + \cdots. \qquad (C8)$$

2. Fully broken O(3) phase

In this case we consider the even spins aligned along the X axis, as in Eq. (C1), while the odd spins are essentially aligned with the Z axis:

$$\vec{\phi}_{\text{odd}} = \left(u_x, u_y, \sqrt{1 - u_x^2 - u_y^2}\right), \qquad (C9)$$

the integration measure being analogous to the one in Eq. (C2). In this case u_x, u_y, v_y, and v_z are all expected to be small at low temperature.

Now the contribution of nearest neighbors to the action is

$$-\frac{1}{T}(\vec{\phi}_{\text{even}} \cdot \vec{\phi}_{\text{odd}})^2 = -\left[\tilde{u}_x\sqrt{1 - \sqrt{T}\tilde{v}_y^2 - T\tilde{v}_z^2} + \tilde{v}_y\tilde{u}_y\right.$$
$$\left. + \tilde{v}_z\sqrt{1 - T\tilde{u}_x^2 - \sqrt{T}\tilde{u}_y^2}\right]^2, \qquad (C10)$$

where, in order to obtain a T-independent contribution, we have needed to use the rescaling $\tilde{u}_y = u_y/\sqrt[4]{T}, \tilde{v}_y = v_y/\sqrt[4]{T}$ and $\tilde{u}_x = u_x/\sqrt{T}, \tilde{v}_z = v_z/\sqrt{T}$. Power expanding in the fields we get

$$(\text{RHS}) = -[\tilde{u}_x + \tilde{v}_z + \tilde{u}_y\tilde{v}_y]^2 + \cdots, \qquad (C11)$$

where the ellipsis stands for terms vanishing at $T=0$. The leading behavior of the partition function with temperature is given by the change of variables: we get a factor $\sqrt{T}$ for $u_x \rightarrow \tilde{u}_x$ (same for v_z) and a factor $\sqrt[4]{T}$ for the change $u_y \rightarrow \tilde{u}_y$ (same for v_y).

Hence, at the leading order in temperature, the partition function is again proportional to $T^{3V/4}$ and the leading singularity of the free energy is exactly as in Eq. (C8).

[1] J. M. D. Coey, M. Viret and S. von Molnar, Adv. Phys. **48**, 167 (1999).

[2] See e.g. E. Dagotto, T. Hotta and A. Moreo, Phys. Rep. **344**, 1 (2001).

[3] E. Dagotto, *Nanoscale Phase Separation and Colossal Magnetoresistance* (Springer-Verlag, Berlin, 2003).

[4] J. M. Carmona *et al.*, Phys. Lett. B **560**, 140 (2003).

[5] See, e. g., D. Amit, *Field Theory, the Renormalization Group and Critical Phenomena* (World Scientific, Singapore, 1984).

[6] C. Zener, Phys. Rev. **82**, 403 (1951); P. W. Anderson and H. Hasegawa, *ibid.* **100**, 675 (1955); P. G. de Gennes, *ibid.* **118**, 141 (1960).

[7] J. A. Verges, V. Martín-Mayor, and L. Brey, Phys. Rev. Lett. **88**, 136401 (2002).

[8] J. L. Alonso, J. A. Capitán, L. A. Fernández, F. Guinea, and V. Martín-Mayor, Phys. Rev. B **64**, 054408 (2001).

[9] J. L. Alonso, L. A. Fernández, F. Guinea, V. Laliena, and V. Martín-Mayor, Phys. Rev. B **63**, 064416 (2001).

[10] J. L. Alonso, L. A. Fernández, F. Guinea, V. Laliena, and V. Martín-Mayor, Phys. Rev. B **63**, 054411 (2001).

[11] J. L. Alonso, L. A. Fernández, F. Guinea, V. Laliena, and V. Martín-Mayor, Nucl. Phys. B **596**, 587 (2001).

[12] S. Kumar and P. Majumdar, cond-mat/0305345 (unpublished).

[13] Shan-Ho Tsai, D. P. Landau, J. Magn. Magn. Mater. **226-230**, 650 (2001); J. Appl. Phys. **87**, 5807 (2000).

[14] S. Sachdev, *Quantum Phase Transitions* (Cambridge University Press, Cambridge, U.K., 1999); Science **288**, 475 (2000).

[15] J. Burgy, M. Mayr, V. Martín-Mayor, A. Moreo, and E. Dagotto, Phys. Rev. Lett. **87**, 277202 (2001).

[16] J. L. Alonso, L. A. Fernández, F. Guinea, V. Laliena, and V. Martín-Mayor, Phys. Rev. B **66**, 104430 (2002).

[17] See E. Dagotto, cond-mat/0302550 (unpublished) and Ref. 3.

[18] H. G. Ballesteros, L. A. Fernández, V. Martín-Mayor, and A. Muñoz Sudupe, Phys. Lett. B **378**, 207 (1996).

[19] H. G. Ballesteros, L. A. Fernández, V. Martín-Mayor, and A. Muñoz Sudupe, Nucl. Phys. B **483**, 707 (1997).

[20] S. Romano, Int. J. Mod. Phys. B **8**, 3389 (1994).

[21] G. Korhing and R. E. Shrock, Nucl. Phys. B **295**, 36 (1988).

[22] S. Elitzur, Phys. Rev. D **12**, 3978 (1975).

[23] S. Uhlenbruck *et al.*, Phys. Rev. Lett. **82**, 185 (1999).

[24] H. Nojiri, K. Kaneko, M. Motokawa, K. Hirota, Y. Endoh, and K. Takahashi, Phys. Rev. B **60**, 4142 (1999).

[25] P. Wagner, I. Gordon, S. Mangin, V. V. Moshchalkov, Y. Bruynseraede, L. Pinsard, and A. Revcolevschi, Phys. Rev. B **61**, 529 (2000).

[26] Shun-Qing Shen, R. Y. Gu, Qiang-Hua Wang, Z. D. Wang, X. C. Xie, Phys. Rev. B **62** 5829 (2000).

[27] P. Azaria, B. Delamotte, and T. Jolicoeur, Phys. Rev. Lett. **64**, 3175 (1990); P. Azaria, B. Delamotte, F. Delduc and T. Jolicoeur, Nucl. Phys. B **408**, 485 (1993).

[28] See, for example, H. Kawamura, Can. J. Phys. **79**, 1447 (2001).

[29] M. Tissier, B. Delamotte, and D. Mouhanna, Phys. Rev. Lett. **84**, 5208 (2000); M. Itakura, J. Phys. Soc. Jpn. **72**, 74 (2003).

[30] A. Pelissetto, P. Rossi, and E. Vicari, Phys. Rev. B **65**, 020403 (2002), and references therein.

[31] B. Cooper, B. Freedman, and D. Preston, Nucl. Phys. B **210**, 210 (1992); J. K. Kim, Phys. Rev. Lett. **70**, 1735 (1993); S. Caracciolo, R. G. Edwardas, A. Pelissetto, and A. D. Sokal, Nucl. Phys. B **403**, 475 (1993).

[32] See, e.g., G. Parisi, *Statistical Field Theory* (Addison-Wesley, New York, 1988).

[33] See De Gennes in Ref. 6.

[34] H. G. Ballesteros and V. Martín-Mayor, Phys. Rev. E **58**, 6787 (1998).

[35] H. G. Ballesteros, L. A. Fernández, V. Martín-Mayor, A. Muñoz Sudupe, G. Parisi, and J. J. Ruiz-Lorenzo, J. Phys. A **32**, 1 (1999).

[36] A. M. Ferrenberg and R. H. Swendsen, Phys. Rev. Lett. **61**, 2635 (1988).

[37] H. G. Ballesteros, L. A. Fernández, V. Martín-Mayor, A. Muñoz Sudupe, G. Parisi, and J. J. Ruiz-Lorenzo, J. Phys. A **32**, 1 (1999).

[38] M. Campostrini, M. Hasenbusch, A. Pelissetto, P. Rossi, and E. Vicari, Phys. Rev. B **63**, 214503 (2001).

[39] M. Hasenbusch, J. Phys. A **34**, 821 (2001).

[40] S. A. Antonenko, and A. I. Sokolov, Phys. Rev. E **51**, 1894 (1995).

[41] L. A. Fernández, M. P. Lombardo, J. J. Ruiz-Lorenzo, and A. Tarancón, Phys. Lett. B **277**, 485 (1992).

[42] A. B. Harris, J. Phys. C **7**, 1671 (1974).

[43] S. Caracciolo and A. Pelissetto, Phys. Rev. E **66**, 016120 (2002).

[44] J. Zinn-Justin, *Quantum Field Theory and Critical Phenomena* (Oxford Science Publications, Oxford, 1990).